

Technische Universität München
Fakultät für Physik



**A thesis submitted in partial fulfillment of the requirements for the
degree of Master of Science in Physics**

Transport Properties of Interacting Edge Modes in 2D Topological Insulators with Random Kondo Impurities

**Transporteigenschaften Wechselwirkender Randzustände von
Zweidimensionalen Topologischen Isolatoren mit Zufälligen
Kondostörstellen**

Ari Wugalter

Wednesday 12th November, 2014

First Supervisor: Prof. Dr. W. Zwerger
Second Supervisor: Prof. Dr. J. von Delft

Contents

1 Quantum Spin Hall Effect	3
1.1 Kane-Mele Model	4
1.2 \mathbb{Z}_2 Topological Invariant	8
2 Edge States of Quantum Spin Hall Insulators	11
2.1 Basic properties of the edge states	11
2.2 Disorder on the edge of a quantum spin Hall insulator	11
2.3 Kondo impurity on the edge of a quantum spin Hall insulator	12
2.4 Conductance of a helical edge state with a Kondo impurity	15
2.5 Array of Kondo impurities on the edge of a quantum spin Hall insulator	18
3 Role of J_z	23
4 Renormalization Group Analysis of Interacting Edge Modes of Topological Insulators with Kondo Impurities	25
4.1 Perturbative renormalization group around a fixed point from operator product expansion	25
4.2 Derivation of the RG equations for the helical edge state with Kondo impurities	29
4.3 Discussion of the RG equations	30
5 Effective Action for the Interacting Edge Mode of Topological Insulators with Kondo Impurities	31
5.1 Construction of a variational free energy functional	31
5.2 Computation of the effective action for the interacting helical edge	32
5.3 Properties of the effective action	33
6 Physics from the effective action	35
6.1 Transport properties of an helical edge state coupled to magnetic impurities from bosonization	35
6.2 Helical edge states at attractive interaction with magnetic impurities	37
6.3 Helical edge states at repulsive interaction with magnetic impurities	38
6.4 Phase diagram of helical edge states with magnetic impurities	39

7 Conclusion, Open questions and Outlook	41
7.1 Conclusion	41
7.2 Open questions	41
A Bosonization of an helical edge state	43
A.1 Construction of a bosonic representation of the Hamiltonian	43
A.2 Bosonic representation of the single-particle operators	46
A.3 Chiral fields $\phi(x)$ and $\theta(x)$	46
A.4 Bosonization of an interacting helical edge state	48
B Giamarchi-Schulz renormalization group	51
C Free energy of the fluctuations of n_z and $\epsilon(x)$ from shift of vacuum energies	55
C.1 Application to the case of isotropically in-plane coupled impurities	55
C.2 Application to the case of anisotropically in-plane coupled impurities	56
Bibliography	59

Acknowledgements

I would like to thank Prof. Zwerger for serving as my advisor at TU Munich and providing me with the opportunity to work on this project at the LMU, as well as, Prof. Jan von Delft for the hospitality of his group. It was my pleasure to work with Oleg Yevtushenko, who introduced me to the problem and guided me through the stages of the project. Further, I would like to express my gratitude to our collaborators Boris Altshuler and Vladimir Yudson. Vladimir Yudson's visit to Munich, last year, provided us with the necessary momentum for the early stages of the project and he supported us constantly with advice, when needed. I am indebted to my officemate Dennis Schimmel for the numerous very helpful discussions about physics and the other members of the von Delft group for making my year with them very enjoyable.

Moreover, I acknowledge useful discussions with Igor Yurkevich, Alexei Tsvetik and Herbert Wagner.

Introduction

Recently, there has been a lot of interest in the physics of systems called topological insulators, which includes the so called quantum spin Hall insulators. These are materials, which are insulating in the bulk, but support gapless modes on the boundary. The presence of time-reversal symmetry in these systems implies a special structure of the edge modes, where spin-up and spin-down particles counterpropagate. Such edge modes are called helical.

The net charge Hall conductance supported by the edge modes vanishes, but the spin Hall conductance is finite. In addition to that, potential disorder can not backscatter electrons, as it is unable to flip their spins. Localization therefore, does not occur in the presence of potential disorder only. In contrast, magnetic impurities can induce backscattering. A recent work by Altshuler et al. considers a non-interacting edge state of a quantum spin Hall insulator with in-plane coupled to Kondo impurities. It is shown, that the conductance is still ideal as long as the coupling between electrons and spins is isotropic in the plane, so that the total s_z component of electrons and spins is conserved. In contrast, it vanishes, if one adds random anisotropy, which breaks the $U(1)$ symmetry of the localized spins and the conservation of the total s_z component.

The aim of this thesis is to generalize the work by Altshuler et al. beyond the conditions given above. Hence, we will add an out-of-plane component of electron-impurity coupling and interactions to the scenario. It will be shown, that a finite out-of-plane coupling can be accounted for, by a change of interaction parameters. A rich phase diagram will be presented, depending on the interaction strength. For weakly attractive or repulsive interactions, the system stays an Anderson insulator, as in the case of absent interactions, which was discussed by Altshuler et al., while for strongly repulsive and strongly attractive interactions, it undergoes insulator-conductor phase transitions. The mechanisms underlying this phase transitions are discussed.

In Chapter 1 we will review the properties of quantum spin Hall insulators. Their edge states and the effect of Kondo impurities on them is the topic in Chapter 2. We will also give an extended recap of the work by Altshuler et al.. In Chapter 3 we will discuss the impact of a finite out-of-plane Kondo coupling J_z , which was

Contents

neglected in the work by Altshuler et al.. Chapter 4 is devoted to an RG analysis of interacting helical edge states with Kondo impurities. The RG analysis will motivate us to establish an effective gapped action for the system, which is developed in chapter 5. The effective action will serve us as a starting point for the discussion of the phase diagram of helical edge modes with Kondo impurities in Chapter 6. We will conclude by outlining further developments and open questions in the final Chapter 7.

Chapter 1

Quantum Spin Hall Effect

The quantum spin Hall effect (QSH) is a close relative of the Integer Quantum Hall Effect (IQHE), which was discovered in the late 1970s.

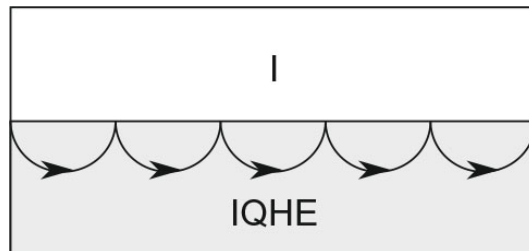


Figure 1.1: Chiral edge states of a quantum Hall device (Source: [16])

Integer quantum Hall effects are observed in 2D electron systems with a perpendicular magnetic field applied, which breaks time-reversal symmetry [20, 9, 34]. The prominent properties of such systems are that they are insulators in the bulk, but still support charge transport via chiral gapless edge states (c.f. figure 1.1). Conductivity is quantized and proportional to a topological invariant of the bulk spectrum, which is known as the TKNN-invariant or first Chern number [33]. It is a topological insulator, because finite, local perturbations of the Hamiltonian like weak interaction and impurities can not alter its physics. Specifically, its chiral edge states are immune to any kind of backscattering and localization by disorder.

Ideal quantum Spin Hall systems are also bulk insulators with gapless edge modes [15, 29, 3, 10]. As opposed to quantum Hall systems, time reversal symmetry is not broken. Therefore, the edge states are not chiral but helical, which means that the direction of the momentum is fixed by the s_z component of the spin. The net charge transport is zero, but a finite quantized spin current is carried. Similarly to the IQHE case, the spin conductivity is connected to a topological invariant of the bulk.

In the following chapter we will describe the first model of a QSH system, which

was proposed by Kane and Mele in 2005 [17]. We will introduce the \mathbb{Z}_2 topological invariant and show how it relates to the spin Hall conductance [18, 30]. Then we are going to argue on the existence of gapless edge states, their properties and the relation to the properties of the bulk. At the end of the chapter we will discuss results on Kondo impurities on edges of QSH insulators, which are important for our further discussion.

1.1 Kane-Mele Model

Kane and Mele realized in 2005 that Graphene with spin-orbit coupling could exhibit a quantum spin Hall effect [17]. Eventually, it turned out that the spin-orbit coupling in graphene is too weak. Nevertheless, we will present it, for it is simple and shows all the features, which are important for a quantum spin Hall device. The first real physical realization of a quantum spin Hall insulator was found to be HgTe-CdTe quantum wells as proposed by Bernevig, Hughes and Zhang [4, 21]. Although the mechanisms that lead to the quantum spin Hall effect are slightly different, the basic principles are shared by both models.

1.1.1 Graphene

A review of the physics of Graphene and Hall effects therein is given in the book by E. Fradkin [9], which is followed in the following sections closely. Graphene is a 2D state of carbon atoms on a honeycomb lattice. One can divide the honeycomb lattice into two triangular sublattices A and B, as shown in the figure. Let $\psi(\mathbf{r}_A)$ and $\chi(\mathbf{r}_A + \mathbf{d}_j)$ be fermionic operators on the A and B sublattices, where \mathbf{d}_j ($j = 1, 2, 3$) are vectors between nearest-neighbor atoms. The simplest tight-binding hamiltonian with nearest neighbor hopping reads

$$H = t \sum_{\mathbf{r}_A, j} \left[\psi^\dagger(\mathbf{r}_A) \chi(\mathbf{r}_A + \mathbf{d}_j) + \text{h.c.} \right] = \quad (1.1)$$

$$= t \sum_{i=j}^3 \int_{\text{BZ}} \frac{d^2\mathbf{k}}{(2\pi)^2} (\psi^\dagger(\mathbf{k}) \quad \chi^\dagger(\mathbf{k})) \begin{pmatrix} 0 & e^{i\mathbf{k} \cdot \mathbf{d}_j} \\ e^{-i\mathbf{k} \cdot \mathbf{d}_j} & 0 \end{pmatrix} \begin{pmatrix} \psi(\mathbf{k}) \\ \chi(\mathbf{k}) \end{pmatrix} = \quad (1.2)$$

$$= t \sum_{j=1}^3 \int_{\text{BZ}} \frac{d^2\mathbf{k}}{(2\pi)^2} (\psi^\dagger(\mathbf{k}) \quad \chi^\dagger(\mathbf{k})) [\cos(\mathbf{k} \cdot \mathbf{d}_j) \sigma_x - \sin(\mathbf{k} \cdot \mathbf{d}_j) \sigma_y] \begin{pmatrix} \psi(\mathbf{k}) \\ \chi(\mathbf{k}) \end{pmatrix}, \quad (1.3)$$

with single-particle energies

$$E_{\pm}(\mathbf{k}) = \pm t \left| \sum_{j=1}^3 e^{i\mathbf{k} \cdot \mathbf{d}_j} \right|. \quad (1.4)$$

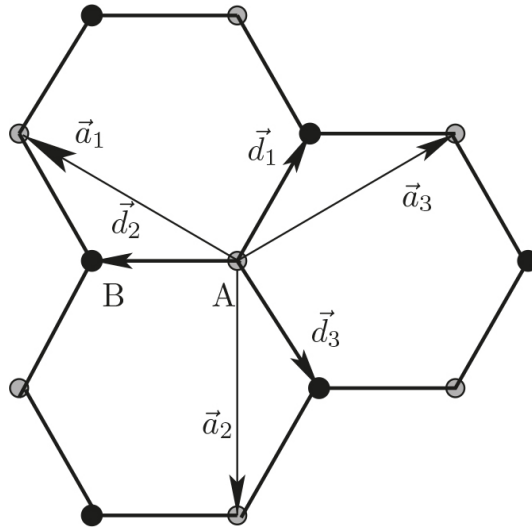


Figure 1.2: Unit cell of Graphene (Source: [9])

Therefore, there are two bands, which meet at two points \mathbf{K} and \mathbf{K}' in the Brillouin zone, where $\sum_{j=1}^3 e^{i\mathbf{K} \cdot \mathbf{d}_j} = 0$.

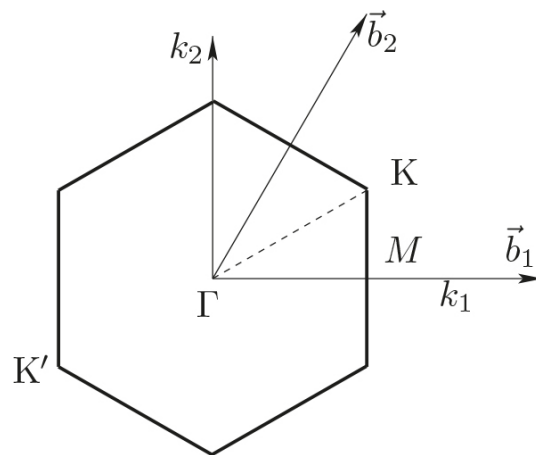


Figure 1.3: Brillouin zone of Graphene (Source: [9])

Near the band crossing points \mathbf{K} and \mathbf{K}' the dispersion relation can be linearized

$$E_{\pm}(\mathbf{q} := \mathbf{k} - \mathbf{K}) = \pm t|\mathbf{q}| \quad (1.5)$$

For charge neutral graphene the Fermi energy is zero. Thus, an effective low

energy theory is obtained by considering only states in the vicinity of K and K'. The Hamiltonian has the form of two Dirac Hamiltonians

$$H = v_F \int \frac{d^2q}{(2\pi)^2} \sum_{\alpha=1,2} \Psi_{\alpha}^{\dagger}(\mathbf{q}) (\sigma_x q_x + \sigma_y q_y) \Psi_{\alpha}(\mathbf{q}), \quad (1.6)$$

where $\Psi_{\alpha}(\mathbf{q})$ are two component spinors. It is important to note that, the absence of terms that are proportional to σ_z , both in the lattice and the continuum Hamiltonian, is a consequence of parity and time-reversal invariance. It is for their presence that forbids having a gap in the band structure and therefore a gap in the Dirac Hamiltonian.

1.1.2 Spin-Orbit Coupling

In 2005 Kane and Mele [17] have realized, that, if one considers spinful fermions with spin-orbit coupling, the effective low energy Dirac Hamiltonian gains a mass term, although preserving time-reversal invariance.

$$H = v_f \int \frac{d^2q}{(2\pi)^2} \sum_{\substack{\alpha=1,2 \\ \sigma, \sigma'=\pm 1}} \Psi_{\alpha, \sigma}^{\dagger}(\mathbf{q}) [(\sigma_x q_x + \sigma_y q_y) \otimes \mathbb{1}] \Psi_{\alpha, \sigma'}(\mathbf{q}) + \Delta \Psi_{\alpha, \sigma}^{\dagger}(\mathbf{q}) [\sigma_z \otimes s^z] \Psi_{\alpha, \sigma'}(\mathbf{q}) \quad (1.7)$$

with

$$\Psi_{1, \sigma} = \begin{pmatrix} \psi_{k, \sigma} \\ \chi_{k, \sigma} \end{pmatrix}, \quad \Psi_{2, \sigma} = \begin{pmatrix} -i\chi_{k, \sigma} \\ i\psi_{k, \sigma} \end{pmatrix}. \quad (1.8)$$

In the next subsection the Hall conductance σ_{xy} for this Hamiltonian will be computed using the Kubo formula. Each spin species contributes with $\sigma_{xy}^{\uparrow, \downarrow} = \pm \frac{e^2}{h}$, which sums to zero (another consequence of time-reversal symmetry) but their difference gives a finite and quantized spin conductance

$$\sigma_{xy}^S = \frac{\hbar}{2e} (\sigma_{xy}^{\uparrow} - \sigma_{xy}^{\downarrow}) = \frac{e}{2\pi}. \quad (1.9)$$

1.1.3 Hall conductance for one spin species

Consider the spin-up component of the Hamiltonian (1.7). It has the general form of a two-level system

$$h(\mathbf{k}) = h_0(\mathbf{k})\mathbb{1} + \sum_{\alpha} h_{\alpha}(\mathbf{k})\sigma_{\alpha}, \quad (1.10)$$

with

$$h_0(\mathbf{k}) = 0 \quad h_1(\mathbf{k}) = q_x \quad h_2(\mathbf{k}) = q_y \quad h_3(\mathbf{k}) = \Delta.$$

The Hall conductance is given by

$$\sigma_{xy} = \lim_{\omega \rightarrow 0} \frac{i}{\omega} \Pi_{xy}(\omega, \mathbf{Q} = 0), \quad (1.11)$$

with the polarization operator

$$\Pi_{xy}(\omega, \mathbf{Q} = 0) = \int \frac{d^2\mathbf{k}}{(2\pi)^2} \int \frac{d\Omega}{2\pi} [J_x(\mathbf{k})G(\mathbf{k}, \omega + \Omega)J_y(\mathbf{k})G(\mathbf{k}, \Omega)], \quad (1.12)$$

where $J_l = \frac{\hbar(\mathbf{k})}{\partial k_l}$ and $G(\mathbf{k}, \omega) = (\omega\mathbb{1} - \hbar(\mathbf{k}) + i\epsilon)^{-1}$.

Using the fact, that we are in an insulator, so that we band with the lower energy is completely filled and the band with the higher energy is completely empty, the expression simplifies to

$$\sigma_{xy} = \frac{e^2}{8\pi^2} \int d^2\mathbf{k} \epsilon^{lmn} \hat{h}_l \partial_{k_x} \hat{h}_m \partial_{k_y} \hat{h}_n, \quad (1.13)$$

where $\hat{h}_i = \frac{\hbar_i}{\|\hbar_i\|}$. The conductance can be recognized to be proportional to a winding number. More precisely, it is the first Chern number N , which characterizes the mapping between the two-dimensional Brillouin zone and the Bloch sphere corresponding to the two-level system. Consequently, the Hall conductances of each of the spin species are topologically quantized [28, 37].

$$\sigma_{xy} = \frac{e^2}{h} N, \quad (1.14)$$

with the first Chern number

$$N = \frac{1}{4\pi} \int d^2\mathbf{k} \epsilon^{lmn} \hat{h}_l \partial_{k_x} \hat{h}_m \partial_{k_y} \hat{h}_n. \quad (1.15)$$

Since $\hbar_0(\mathbf{k}) \rightarrow -\hbar_0(\mathbf{k})$, for from the spin-down part of the Hamiltonian, it's contribution to the conductance has equal magnitude, but opposite sign compared to the contribution from the spin-up part of the Hamiltonian. Therefore, the total charge conductance is equal to zero, but the spin conductance is finite and topologically quantized.

1.2 \mathbb{Z}_2 Topological Invariant

In the previous chapter, the simple Kane-Mele model of a quantum spin Hall device was presented. It can be understood as a combination of two quantum Hall devices, one for each spin species, with opposite Hall conductances. It was seen, that the Hall conductance of each of the quantum Hall devices could be computed using a topological bulk invariant. The total Chern number of the two spin species is always equal to zero, reflecting the absence of total charge conductance and therefore not a good characteristic for the system. Nevertheless, one can expect the existence of a topological invariant, which discriminates quantum spin Hall insulators, which have edge states, that are protected from finite, local perturbations from topologically trivial insulators, which don't have them. Further, it will be argued, that as opposed to quantum Hall insulators, that are characterized by an integer, for time-reversal invariant insulators it makes only sense to distinguish two different states. Hence, we have a \mathbb{Z}_2 instead of a \mathbb{Z} classification.

1.2.1 Time-Reversal Invariance

In order to understand the appearance of a \mathbb{Z}_2 topological invariant, one needs to gain deeper insight into time-reversal symmetry. For a single spin-1/2 particle the time-reversal operator has the form [16]

$$\Theta = \exp(i\pi\sigma) K, \quad (1.16)$$

where K is the complex conjugation operator. Θ has the important property

$$\Theta^2 = -1. \quad (1.17)$$

We consider a time-reversal invariant Bloch Hamiltonian

$$H(\mathbf{k}) = e^{-i\mathbf{k}\cdot\mathbf{r}} \mathcal{H} e^{i\mathbf{k}\cdot\mathbf{r}}, \quad (1.18)$$

so that the single-particle Hamiltonian \mathcal{H} satisfies $[\mathcal{H}, \Theta] = 0$, which implies

$$\Theta H(\mathbf{k}) \Theta^{-1} = H(-\mathbf{k}). \quad (1.19)$$

Condition (1.17) requires each eigenstate of the Hamiltonian to be degenerate. To prove this let us for a moment assume, that there is an eigenstate $|\chi\rangle$, which is non-degenerate. As $\Theta|\chi\rangle$ must also be an eigenstate of the Hamiltonian,

$$\Theta|\chi\rangle = c|\chi\rangle \quad (1.20)$$

must hold for $|\chi\rangle$. Further, equations (1.17) and (1.20) require

$$|c|^2 = \langle\chi|\Theta|\Theta\chi\rangle = \langle\chi|\Theta^2|\chi\rangle = -1, \quad (1.21)$$

which is a contradiction. This special kind of degeneracy is called Kramers degeneracy. For systems without spin-orbit coupling, Kramers degeneracy is equivalent to the degeneracy between spin-up and spin-down states, while for systems including spin-orbit coupling it is more intricate.

1.2.2 Bulk-Boundary Correspondence

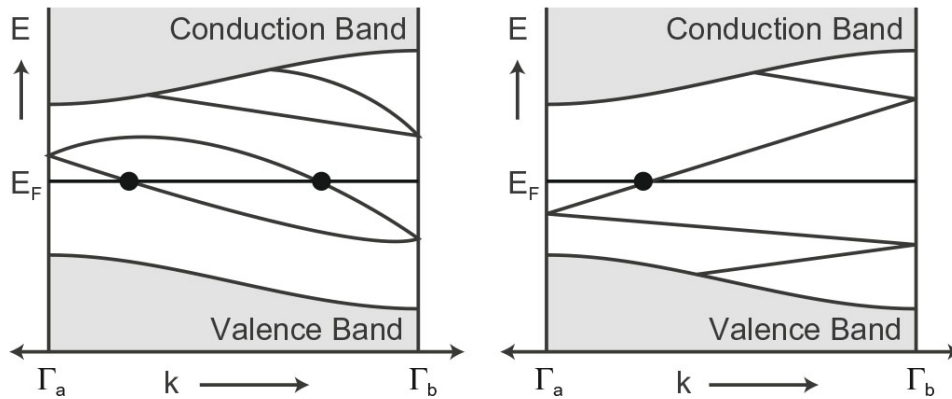


Figure 1.4: Electronic dispersion between two boundary Kramers degenerate points. In the left the number of surface states crossing the Fermi energy is even, whereas in the right panel it is odd. (Source: [10])

Figure 1.4 shows two halves of Brillouin zones ($\Gamma_a = 0 < k_x < \frac{\pi}{a} = \Gamma_b$) of time-reversal invariant two-dimensional insulators. Considering only one half is sufficient, since the other half is the mirror images of the first one due to time-reversal invariance, with partners of Kramers pairs being reflected on each other. The shaded regions show the bulk conduction and valence bands, which are separated by a gap. Besides, it is assumed, that the system has edge states inside the gap. The aforementioned mirror symmetry requires the Kramers partners to connect at the points at the borders of the half of the Brillouin zone Γ_a and Γ_b . The connection can occur twofold. Either the Kramers pairs connect pairwise, as in the left panel, so that all edge states can be pulled below the chemical potential by shifting it, or, as in the right panel the edge states connect to cross the bulk gap. The first case is equivalent to absence of any edge states, while the second corresponds to the existence of topologically protected edge states, vulgo a quantum spin Hall insulator. From another perspective, we see, that the topologically trivial and non-trivial cases are distinguished by whether the chemical potential crosses the bands an even or an odd number of times. We can therefore define ν , the \mathbb{Z}_2 topological invariant for time-reversal invariant insulators as the

parity of Kramers pairs crossing the bulk gap [16],

$$\nu = N_k \pmod{2}. \quad (1.22)$$

Chapter 2

Edge States of Quantum Spin Hall Insulators

2.1 Basic properties of the edge states

For the quantum Hall insulator the edge states are chiral [9, 34], which means that the direction of the edge electrons is determined by the magnetic field. The quantum spin Hall insulator as realised in the Kane-Mele model can be understood as two copies of a quantum Hall insulator, one for each spin component, with opposite Hall conductances. Thus, the edge mode of the quantum spin Hall insulator consists of two gapless Dirac fermions that have opposite spin and are counterpropagating. It was dubbed "helical" by Wu et al.. For the Bernevig-Hughes-Zhang [4] model this picture of edge states was confirmed explicitly analytically and numerically [29]. Realistic models of quantum spin Hall insulators usually have additional Rashba spin-orbit coupling which breaks conservation of s_z component of the spin. Still, most properties that hold for the ideal quantum spin Hall edge states, can be shown to hold also for edges with Rashba spin-orbit coupling.

2.2 Disorder on the edge of a quantum spin Hall insulator

Consider impurities without internal degrees of freedom on the edge of a quantum spin Hall insulator. As discussed in the previous section, in a perfect quantum spin Hall insulator edge mode, left moving and right moving particles have opposite spin, so that for such disorder backscattering is impossible and, thusly edge states can not be localized. A more general argument from the symmetry properties of S-matrices was given by Kane and Mele [?, 16].

They consider an edge state, which is disordered in a finite region. The solution of the scattering problem can be expressed in terms of an S-matrix which maps the incoming on the outgoing states

$$\Phi_{\text{in}} = S\Phi_{\text{out}}, \quad (2.1)$$

where $\Phi = (\phi_L \ \phi_R)^T$ is a spinor of left- and right-movers.

As was mentioned in the previous chapter, the time-reversal operator for spin-1/2 particles has the form

$$\theta = \exp(i\pi\sigma_y)K. \quad (2.2)$$

Time-reversal invariance demands the S-matrix to satisfy

$$S = \sigma_y S^T \sigma_y, \quad (2.3)$$

from which it is straightforward to deduce, that the S-matrix has no off-diagonal elements which would correspond to backscattering.

Nethertheless, if the impurities have a spin-structure, the form of the time-reversal operator changes, so that the argument above breaks down and backscattering becomes possible.

2.3 Kondo impurity on the edge of a quantum spin Hall insulator

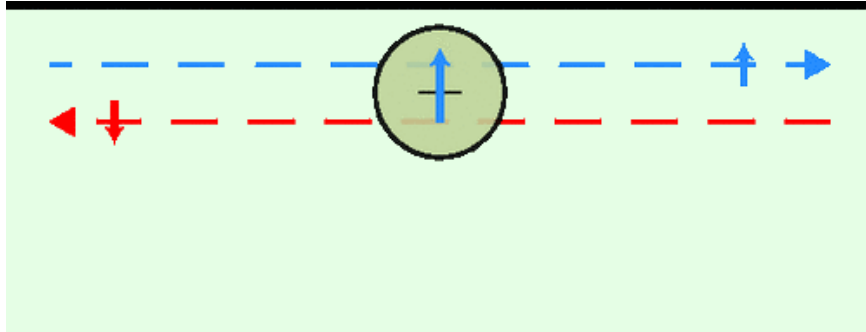


Figure 2.1: Kondo impurity on the edge of a quantum spin Hall insulator (Source: PRB 84 195310 (2011))

The problem of a Kondo impurity on the edge of a quantum spin Hall insulator was first considered by Wu et al. [35]. Later Maciejko et al. [25] have given an extended review of its physics. Consider a bosonized Hamiltonian of the helical edge

$$H_{TL} = \frac{1}{2\pi} \int dx \left[uK (\partial_x \theta)^2 + \frac{u}{K} (\partial_x \phi)^2 \right] \quad (2.4)$$

and a Kondo impurity at $x = 0$ coupled to it

$$H_K = \frac{J_{\perp} a}{2\pi\xi} \left[S^+ e^{-i2\phi(0)} + \text{h.c.} \right] - \frac{J_z a}{\pi} S^z \partial_x \theta(0). \quad (2.5)$$

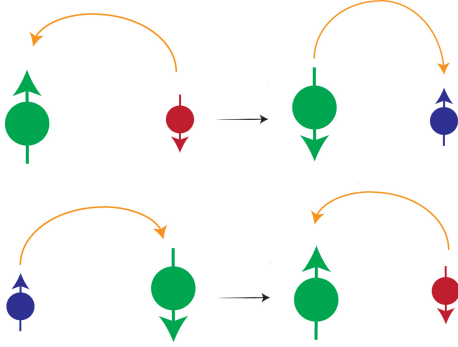


Figure 2.2: Backscattering is only possible with a flip of the spins of the electron and the impurity

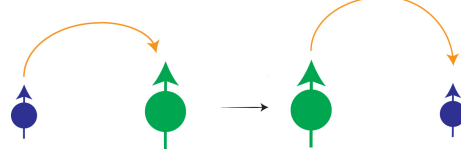


Figure 2.3: Forward scattering is only possible without flipping any spins

The first part in the Kondo term of the Hamiltonian correspond to spin-flip backscattering (c.f. figure 2.2), whereas the second term describes forward scattering with conserved spin (cf. figure 2.3). Other processes are not compatible with the helical structure of the edge. In particular, there is no spin-flip forward scattering in a helical liquid.

The one-loop RG equation's for the Kondo model in a helical edge state read

$$\frac{dJ_{\perp}}{dl} = (1 - K)J_{\perp} + J_{\perp}J_z \quad (2.6)$$

$$\frac{dJ_z}{dl} = J_{\perp}^2, \quad (2.7)$$

which can be understood as type of anisotropic Kondo model [12] with J_z shifted to $J_z + 1 - K$.

The Kondo temperature has the form

$$T_K = D \exp\left(-\frac{1}{J_{\perp}} \frac{\sinh^{-1} \alpha}{\alpha}\right), \quad (2.8)$$

where $\alpha = \left[\left(\frac{J_z + 1 - K}{J_{\perp}}\right)^2 - 1\right]^{\frac{1}{2}}$ is an anisotropy parameter. It shows two characteristic regions, depending on whether $\alpha^2 \lesssim 0$ or $\alpha^2 \gg 0$. In the first case it has the exponential form known from the regular Kondo model

$$T_K = D \exp\left(-\frac{1}{J_{\perp}}\right), \quad (2.9)$$

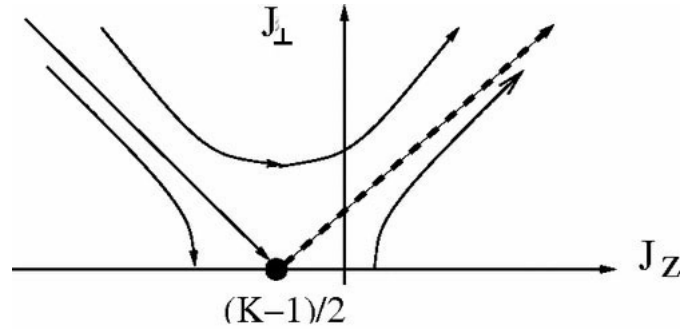


Figure 2.4: RG flow of the Kondo model in a helical edge state (Source:[35])

while in the latter case its form resembles the Kondo temperature of the spinful Luttinger Kondo model [23, 11]

$$T_K = D \left(\frac{J_{\perp}}{1-K} \right)^{\frac{1}{1-K}}. \quad (2.10)$$

As shown in figure 2.4 for weak ferromagnetic and anti-ferromagnetic couplings the system flows to a Kondo singlet fixed point (c.f. figure 2.5). For a Luttinger

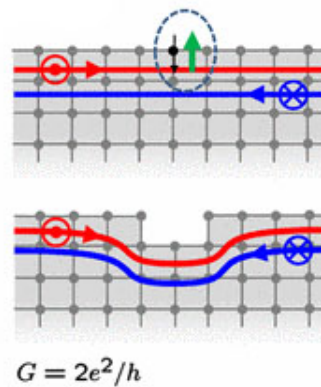


Figure 2.5: Physical picture of the Kondo singlet fixed point in a helical edge state (Source: [25])

liquid one would expect, that conductance through the Kondo singlet is impossible [11]. However, as spin-flip backscattering of a spin-1/2 electron from the spin-0 Kondo singlet is impossible, conductance is not affected by the screened impurity. It decouples from the helical edge state [25] and ideal conductance is restored (c.f. figure 2.5).

2.4 Conductance of a helical edge state with a Kondo impurity

The conductance through a helical edge state with a Kondo impurity was first discussed by Maciejko et al. [25] for the case of dc conductance and was later revised and expanded to finite frequencies by Tanaka et al. [32]. In this section, we will follow the paper by Tanaka et al..

The Hamiltonian has the same form as in the previous section plus an additional source term, which couples to the spin density $\partial_x \theta$

$$H = H_{TL} + H_K - \frac{eV}{2\pi} \int dx \partial_x \theta(x). \quad (2.11)$$

The source term assigns different chemical potentials to the left- and right moving particles. One can achieve the same effect by introducing an effective magnetic field which is applied to the Kondo impurity

$$H_V = -eVS^z. \quad (2.12)$$

Qualitatively this substitution can be justified, because as long as the z component of the total spin of the system is conserved, one can use the localized impurity as a counter for scattering processes in the system. Forward scattering does not influence the spin conductance and can therefore be neglected. Each backscattering of an electron is accompanied by a flipping of the magnetic impurity. The energy cost of a backscattering cost is either due to the difference in chemical potentials, if we use the former type of source term or due to one configuration of the Kondo impurity being more favorable than the other, with the latter form of the source term. More formally, one can justify the equivalence of the two terms by seeing, that their difference commutes with the Hamiltonian. It is convenient to rescale the fields by \sqrt{K} and to eliminate the J_z -dependent term from the Hamiltonian using the transformation operator $U = e^{i \frac{J_z}{\pi u \sqrt{K}} \Phi(x) S^z}$, so that the effects of both are described by a common parameter $\tilde{K} = K \left(1 - \frac{J_z}{2\pi u \sqrt{K}}\right)^2$.

Using the qualitative picture provided above we can compute the correction to the conductance due to backscattering of electrons off the impurity. The correction to the current is given by

$$\delta I = -e \partial_t S^z = \frac{ieJ_\perp}{2\pi\xi} \left[S^+ e^{i2\sqrt{\tilde{K}}\Phi(0)} - \text{h.c.} \right]. \quad (2.13)$$

Using Kubo formula the correction to the conductance can be evaluated to lowest

order in J_{\perp} to be

$$\delta G(\omega) = -2e^2 \left(\frac{J_{\perp}}{2\pi\xi} \right)^3 \left(\frac{\pi T}{D} \right)^{2\tilde{K}} \sin(\pi\tilde{K}) \times \\ \times \frac{1}{i\omega} \int_0^{\infty} dt \frac{e^{i\omega t} - 1}{[\sinh(\pi T t)]^{2\tilde{K}}}. \quad (2.14)$$

In the low frequency limit $\omega \ll T$ the formula above simplifies to

$$\delta G = -\frac{e^2 \gamma_0}{2T}, \quad (2.15)$$

where

$$\gamma_0 = J_{\perp}^2 \gamma \quad \gamma = \frac{[\Gamma(\tilde{K})]^2}{(2\pi)^2 \xi u \Gamma(2\tilde{K})} \left(\frac{2\pi T}{D} \right)^{2\tilde{K}-1}. \quad (2.16)$$

The parameter γ_0 can be understood as the rate of spin-flips of the Kondo impurity at zero voltage bias. In the paper by Maciejko et al. the same result was derived by a similar approach. However, one must pay attention to the fact, that the formula is perturbative in J_{\perp} . Hence, it describes well the physics in the limit $T \gg \omega \gg \gamma_0 \propto J_{\perp}^2$, where the dynamics of the impurity is dominated by the ac driving voltage, but deviations are observed in the limit $\omega \ll \gamma_0$, where the spin persists for a long time in one of the configurations.

To account more properly for this regime, one can make an augmented ansatz for the dynamics of the impurity. Denote therefore by P_{\uparrow} and P_{\downarrow} the probabilities of the localized spin to be in its up- or down state, respectively. The time-evolution of the probabilities is governed by a rate equation

$$\partial_t P_{\uparrow} = \gamma_+ P_{\downarrow} - \gamma_- P_{\uparrow}, \quad (2.17)$$

where γ_{\pm} are the transition rates between the states. Besides, the probabilities suffice conservation of total probability $P_{\uparrow} + P_{\downarrow} = 1$ at all times. For small voltages $eV \ll T$, the transition rates are given by

$$\gamma_{\pm} = \gamma_0 \left(1 \pm \frac{eV}{2T} \right). \quad (2.18)$$

Analogously to the discussion above, the correction to the current is $\partial I = -e \partial_t P_{\uparrow}$ and the correction to the conductance is $\delta G(\omega) = \frac{\delta I}{V}$, where $V = V_0 e^{i\omega t}$. Solving the rate equations yields a correction to the conductivity of the form

$$\delta G(\omega) = -\frac{e^2 \gamma_0}{2T} \frac{\omega}{\omega + 2i\gamma_0}. \quad (2.19)$$

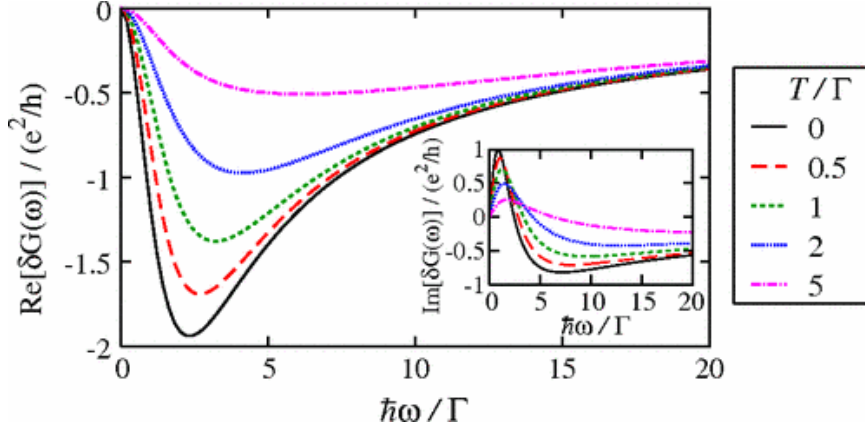


Figure 2.6: Real and imaginary parts of correction to conductance at different temperatures (Source: [32])

The correction of the correction to the conductance is plotted against the frequency for several different temperatures in figure 2.6. As predicted, one retrieves the perturbative result from Equation (2.15) on the preceding page in the limit $\gamma_0 \ll \omega \ll T$, while in the dc limit the correction to the conductance goes down to zero. This is in accordance to the qualitative picture, because in this limit for every left moving particle, that is backscattered, there is exactly one right moving particle, that is backscattered subsequently, so that the total number of left- and right movers is conserved. This is true as long as the in-plane Kondo coupling is isotropic. Anisotropic in-plane Kondo coupling ($J_x \neq J_y$) breaks the conservation of the z -component of the total spin, so that a finite correction to the dc conductance can be obtained from the rate equation

$$\delta G = -\frac{e^2 \gamma_0 (J_x - J_y)^2 (J_x + J_y)^2}{2T (J_x^2 + J_y^2)}. \quad (2.20)$$

The qualitative picture can be expected to hold beyond the region, where the rate equation applies, but it breaks down for $T \ll T_K$, where the Kondo impurity become screened and can not be spin-flipped by electrons any more. As mentioned in the previous section, a Kondo singlet decouples from the helical liquid and the correction to the conductance vanishes.

2.5 Array of Kondo impurities on the edge of a quantum spin Hall insulator

2.5.1 Isotropically in-plane coupled impurities

In the last section we outlined the properties of edge states of quantum spin Hall insulators with Kondo impurities. In a recent paper Altshuler et al. [2] went one step further by considering a non-interacting helical edge state with a distribution of Kondo impurities and discussed the transport properties of such systems. The impurities and the edge state are assumed to be coupled only in-plane ($J_z = 0$, $J_\perp \neq 0$). The system, which is at zero temperature, is described by the Matsubara

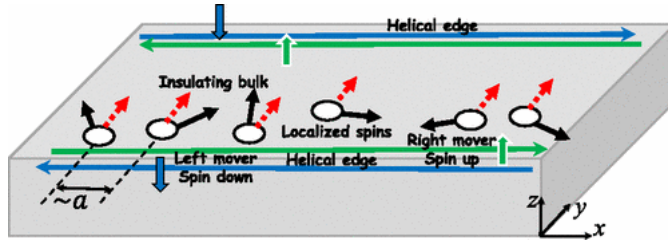


Figure 2.7: Localized magnetic impurities interact with edge states of a quantum spin Hall insulator (Source: [2])

action

$$S = \int dx d\tau (\bar{\Psi}_L \quad \bar{\Psi}_R) \begin{pmatrix} \partial_+ + h(x, \tau) & \Delta(x) \sqrt{1 - n_z^2} e^{-i\alpha} \\ \Delta(x) \sqrt{1 - n_z^2} e^{i\alpha} & \partial_- + h(x, \tau) \end{pmatrix} \begin{pmatrix} \psi_L \\ \psi_R \end{pmatrix} + S_{WZ} \quad (2.21)$$

$$S_{WZ} = -i \int dx d\tau \rho(x) n_z(x, \tau) \partial_\tau \alpha(x, \tau) \quad (2.22)$$

where S_{WZ} is the Wess-Zumino term, where we assumed $\alpha(x, \tau)$ to be smooth, $h(x, \tau)$ is a source field, the localized spins are parametrized by $S^z(x, \tau) = S n_z(x, \tau)$ and $S^\pm(x, \tau) = S \sqrt{1 - n_z^2(x, \tau)} e^{\pm i 2k_F x} e^{\pm i \alpha(x, \tau)}$ and $\Delta(x) = S \rho(x) J_\perp$, where $\rho(x)$ is the density distribution of the impurities. The phase $e^{i 2k_F x}$ comes originally from the electrons and is here included in the definition of the spins. It can be absorbed into a redefinition of $\alpha(x, \tau)$, as long as one is not interested in the exact type of ordering of the spins. The action has the form of gapped Dirac fermions, so one is tempted to believe, that transport through these systems is suppressed. Altshuler et al. have shown, that this is not the case, but an ideal conductance is supported by composite electron-spinon excitation. To see this a gauge transformation is

2.5 Array of Kondo impurities on the edge of a quantum spin Hall insulator

performed, which couples electron and spin degrees of freedom

$$\psi_R \rightarrow e^{-i\alpha(x,\tau)/2}\psi_R \quad (2.23)$$

$$\psi_L \rightarrow e^{i\alpha(x,\tau)/2}\psi_L. \quad (2.24)$$

Thereby the action gains an additional term from the chiral anomaly

$$S_{\text{an}} = \frac{v_F}{8\pi} \int dx d\tau (\partial_x \alpha)^2 - \frac{1}{2\pi} \int dx d\tau h(x, \tau) \partial_x \alpha \quad (2.25)$$

and the total action reads

$$S = \int dx d\tau (\bar{\psi}_L \quad \bar{\psi}_R) \begin{pmatrix} \partial_+ - \frac{i}{2} \partial_+ \alpha(x, \tau) + h(x, \tau) & \Delta(x) \sqrt{1 - n_z^2} \\ \Delta(x) \sqrt{1 - n_z^2} & \partial_- + \frac{i}{2} \partial_- \alpha(x, \tau) + h(x, \tau) \end{pmatrix} \begin{pmatrix} \psi_L \\ \psi_R \end{pmatrix} + S_{\text{WZ}} + S_{\text{an}}. \quad (2.26)$$

2.5.2 Separation of lengthscales

The electrons are mediating an effective interaction between the Kondo impurities, known as RKKY interaction [19]. It can be obtained as first order perturbation correction of the energy in the exchange coupling. For Kondo impurities in an helical edge state, which are only coupled in-plane ($J_z = 0, J_\perp \neq 0$) it has the form

$$H_{\text{RKKY}} = -\frac{J_\perp^2}{8\pi v_F} \frac{S^+(x_j)S^-(x_l)e^{i2k_F(x_j-x_l)} + S^-(x_l)S^+(x_j)e^{-i2k_F(x_j-x_l)}}{|x_j - x_l|}. \quad (2.27)$$

The RKKY interaction induces an ordering of the spins in the $x - y$ -plane, as long as it dominates Kondo screening of the impurities. For non-interacting edge-states this is a valid assumption, because the characteristic energy scale, which describes Kondo screening, the Kondo temperature is smaller than the energy scale of the exchange interaction. The variables corresponding to the ordered spins $\alpha(x, \tau)$ and $n_z(x, \tau)$ are considered to be slow, varying on lengthscales much larger than the electron coherence length $\frac{v_F}{\Delta}$, while the gapped fermionic fields vary on short distances, which are much smaller than that. Hence, one can assume the spin

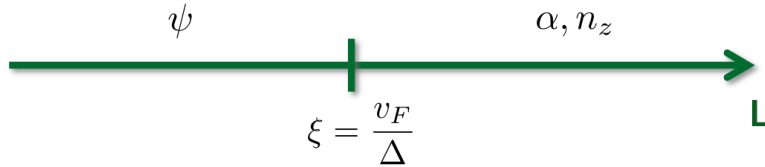


Figure 2.8: Ordering of the Kondo impurities by electronically mediated exchange interactions, induce a separation of lengthscales

variables to attain a constant average value during calculations with the fermionic fields.

2.5.3 Effective action for $\alpha(x, \tau)$

Using the separation of scales one can integrate out the gapped fermionic modes and derive an effective action for n_z . Hence, the part of the action, which describes the interaction between electrons and impurities, is divided in two parts, one of which is independent of n_z and the other depends on n_z

$$S_{e\text{-imp}} = S_{n_z=0} + \delta S, \quad (2.28)$$

$$S_{n_z=0} = \int dx d\tau (\bar{\Psi}_L \quad \bar{\Psi}_R) \begin{pmatrix} \partial_+ & \Delta(x) \\ \Delta(x) & \partial_- \end{pmatrix} \begin{pmatrix} \psi_L \\ \psi_R \end{pmatrix}$$

$$\delta S = \int dx d\tau (\bar{\Psi}_L \quad \bar{\Psi}_R) \begin{pmatrix} 0 & \Delta(x) (\sqrt{1-n_z^2}-1) \\ \Delta(x) (\sqrt{1-n_z^2}-1) & 0 \end{pmatrix} \begin{pmatrix} \psi_L \\ \psi_R \end{pmatrix}, \quad (2.29)$$

where we left out the source and neglected gradients of α , which are small compared to gradients of ψ , due to separation of scales.

Integrating out the fermions gives a functional determinant, which can be reexponentiated

$$\text{tr log } G_{e\text{-imp}}^{-1} = \quad (2.30)$$

$$= \text{tr log} \left[\underbrace{\begin{pmatrix} \partial_+ & \Delta(x) \\ \Delta(x) & \partial_- \end{pmatrix}}_{G_{n_z=0}^{-1}} + \underbrace{\begin{pmatrix} 0 & \Delta(x) (\sqrt{1-n_z^2}-1) \\ \Delta(x) (\sqrt{1-n_z^2}-1) & 0 \end{pmatrix}}_{\delta G^{-1}} \right] =$$

$$= \text{tr log } G_{n_z=0}^{-1} + \text{tr log} (\mathbb{1} + G_{n_z=0} \delta G^{-1}). \quad (2.31)$$

The latter term can be expanded to quadratic order in n_z

$$\text{tr log} (\mathbb{1} + G_{n_z=0} \delta G^{-1}) \approx \text{tr log } G_{n_z=0} \delta G^{-1} \approx \quad (2.32)$$

$$\approx -\Delta^2(x) \int \frac{d\omega d\mathbf{q}}{(2\pi)^2} \frac{1}{\omega^2 + (v_f \mathbf{q})^2 + \Delta^2(x)} n_z^2 =$$

$$= \frac{1}{2\pi v_F} \Delta^2(x) \log \left(\frac{D}{\Delta(x)} \right) n_z^2, \quad (2.33)$$

where D is an ultra-violet cut-off, which corresponds to the gap in the bulk of the quantum spin Hall insulator. By restoring the integrations over long lengthscales we receive an effective action for $n_z(x, \tau)$, which reads

$$S_{n_z} = \frac{1}{2\pi v_F} \int dx d\tau \Delta^2(x) \log \left(\frac{D}{\Delta(x)} \right) n_z^2. \quad (2.34)$$

2.5 Array of Kondo impurities on the edge of a quantum spin Hall insulator

The sign of the effective contribution to the action from $n_z(x, \tau)$ reassures, that the assumption of n_z being small and its fluctuations suppressed, was correct.

It is then possible to integrate out $n_z(x, \tau)$, which leads to an effective action for $\alpha(x, \tau)$

$$S_{\text{eff}} = \frac{1}{2\pi u K} \int dx d\tau \left[(\partial_\tau \alpha)^2 + u^2 (\partial_x \alpha)^2 \right] - \frac{1}{2\pi} \int dx d\tau h(x, \tau) \partial_x \alpha, \quad (2.35)$$

where $u = \frac{\Delta}{2\pi S \bar{\rho}} \sqrt{\log\left(\frac{D}{\Delta}\right)}$ and $K = 4 \frac{u}{v_F}$. Note, that $K = \frac{2\sqrt{\log\left(\frac{D}{\Delta}\right)} \frac{1}{\bar{\rho}}}{\pi S \xi} \ll 1$, because the coherence length of the electrons ξ is much greater than the average distance between the electrons $\frac{1}{\bar{\rho}}$.

The effective action described by equation (2.35) has the form of a strongly repulsive ($K \ll 1$) Luttinger liquid [12], with the source field $h(x, \tau)$, which was initially coupled to the electron density, now coupled to $\partial_x \alpha(x, \tau)$. By taking variational derivatives, one can derive the conductance of the system

$$\sigma(\omega) = \frac{ie^2 v_F u^2}{2\pi\omega v_F^2}, \quad (2.36)$$

which corresponds to ballistic conductance, with a drude weight of $\frac{u^2}{v_F^2}$. The dielectric response contribution from the fermionic determinant (2.31) was neglected, because it vanishes in the limit of small frequencies.

2.5.4 Anisotropically in-plane coupled impurities

The physics changes drastically, if one introduces random anisotropy to the coupling between electrons and impurities. The modified action has the form

$$S = \int dx d\tau (\bar{\Psi}_R, \bar{\Psi}_L) \begin{pmatrix} \partial_+ \\ \sqrt{1 - n_z^2} \Delta(x) e^{i\alpha} [1 + \epsilon^*(x) e^{-i2\alpha}] \end{pmatrix} \begin{pmatrix} \sqrt{1 - n_z^2} \Delta(x) e^{-i\alpha} [1 + \epsilon(x) e^{i2\alpha}] \\ \partial_- \end{pmatrix} \begin{pmatrix} \Psi_R \\ \Psi_L \end{pmatrix}. \quad (2.37)$$

Apparently, introducing such anisotropic couplings is tantamount to breaking the conservation of the total z -component of spin. Following the steps from above, one can derive an effective action for $\alpha(x, \tau)$ with an additional correction from the random anisotropy

$$S_{\text{eff}} = \frac{1}{2\pi u K} \int dx d\tau \left[(\partial_\tau \alpha)^2 + u^2 (\partial_x \alpha)^2 \right] - \frac{1}{v_F} \int dx d\tau \mathcal{E}^2(x) \cos [2\alpha(x, \tau) - \gamma(x)], \quad (2.38)$$

where $\mathcal{E}^2 = \bar{\rho}^2 \pi u^2 |\epsilon(x)|$ and $\gamma(x) = \arg[\epsilon(x)]$.

In contrast to the effective action for $\alpha(x, \tau)$ in the isotropic case (equation (2.35) on the previous page), which corresponded to a strongly repulsive clean Luttinger liquid, the effective action in the anisotropic case (equation (2.38) on the preceding page) describes a strongly repulsive disordered Luttinger liquid. Giamarchi and Schulz [13] have shown, that such a system is an Anderson insulator, specifically the dc conductance $\sigma(\omega \rightarrow 0) = 0$ vanishes, which is again in stark contrast to the case of isotropic couplings. A brief review of their work can be found in the appendix.

Chapter 3

Role of J_z

We are using the work by Altshuler et al. as starting point for a discussion of transport properties of edge states of quantum Hall insulators with Kondo impurities. Hence, we are going to investigate the ramifications of their assumptions and generalize the result beyond these.

The first assumption, that was made, is that out-of plane coupling of electrons and localized spins can be safely disregarded without altering significantly the physics. Let us therefore consider the bosonized Hamiltonian of an interacting helical edge state with embedded magnetic impurities, described by a impurity density $\rho(x)$

$$H = \underbrace{\frac{1}{2\pi} \int dx \left[uK (\partial_x \theta)^2 + \frac{u}{K} (\partial_x \phi)^2 \right]}_{H_{TL}} - \frac{J_z}{\pi} \int dx \rho(x) S^z \partial_x \theta + \frac{J_{\perp}}{2\pi} \int dx \rho(x) \left[S^+ e^{-i2\phi(x)} + \text{h.c.} \right]. \quad (3.1)$$

Further, we will assume, for the sake of simplicity, the impurity distribution to be point-like of the form $\rho(x) = \sum_{b=1}^{N_{\text{imp}}} \delta(x - x_b)$, where x_b are the positions of the impurities. This can be done, since we can represent any continuous distribution as a limit of such point-like distributions.

Consider the unitary operator, which was first proposed for such systems by Maciejko in [24]

$$U = \exp \left[i\lambda \sum_{b=1}^{N_{\text{imp}}} \phi(x_b) S^z \right], \quad (3.2)$$

where λ is a real parameter, to be chosen a posteriori. It induces the following

transformation properties

$$Uf[\phi(x), \partial_x \phi(x), \dots] U^\dagger = f[\phi(x), \partial_x \phi(x), \dots] \quad (3.3)$$

$$U[\nabla\theta(x)]^2 U^\dagger = [\nabla\theta(x)]^2 - 2\lambda S^z \pi \nabla\theta(x) \sum_{b=1}^{N_{\text{imp}}} \delta(x - x_b) \quad (3.4)$$

$$US^z U^\dagger = S^z \quad (3.5)$$

$$US^\pm U^\dagger = S^\pm e^{\pm i\lambda\phi(x)}. \quad (3.6)$$

Thus, the Hamiltonian (3.1) transforms as

$$UHU^\dagger = H_{\text{TL}} - \frac{J_z + \lambda u K \pi}{\pi} \int dx \rho(x) S^z \partial_x \theta + \frac{J_\perp}{2\pi} \int dx \rho(x) \left[S^+ e^{-i2(1-\frac{\lambda}{2})\phi(x)} + \text{h.c.} \right]. \quad (3.7)$$

To proceed further in our analysis we can pick $\lambda = -\frac{J_z}{uK\pi}$ and rescale

$$\left(1 + \frac{J_z}{2\pi u K}\right) \phi(x) \rightarrow \phi(x) \quad (3.8)$$

$$\left(1 + \frac{J_z}{2\pi u K}\right) K \rightarrow \tilde{K} \quad \left(1 + \frac{J_z}{2\pi u K}\right)^{-1} u \rightarrow \tilde{u} \quad uK = \text{const.}, \quad (3.9)$$

so that the transformed Hamiltonian has the form

$$\tilde{H} = \frac{1}{2\pi} \int dx \left[uK (\partial_x \theta)^2 + \frac{\tilde{u}}{\tilde{K}} (\partial_x \phi)^2 \right] + \frac{J_\perp}{2\pi} \int dx \rho(x) \left[S^+ e^{-i2\phi(x)} + \text{h.c.} \right]. \quad (3.10)$$

The transformed Hamiltonian can again be understood as an interacting helical edge with Kondo impurities, which now couple via their in-plane spin components only. During the transformation interaction parameters K and u are altered. In other words, it is possible to map an Hamiltonian with in- and out-of-plane couplings between electrons and spins to an Hamiltonian with in-plane couplings only, but with different strength of electron-electron interactions. Moreover, tuning the out-of plane coupling strength J_z is shown to be equivalent to tuning the interaction strength. As will be shown in the following chapters, finite interactions can significantly change the transport of the edge state and so does a finite J_z . Therefore, the assumption of J_z being negligible is in general not justified.

Chapter 4

Renormalization Group Analysis of Interacting Edge Modes of Topological Insulators with Kondo Impurities

4.1 Perturbative renormalization group around a fixed point from operator product expansion

Special properties of RG fixed points, give rise to elegant methods for the derivation of RG flow equations around them. We will follow the books by J. Cardy and E. Fradkin [5, 9] for the development of the method, which will be applied to our problem in the next section.

4.1.1 Conformal symmetry

A system at a fixed points of the renormalization group (RG) is scale invariant, which means that the actions does not change under RG transformations. Hence, there can be no finite length scales for the system at a RG fixed point, specifically, the correlation length ξ is either infinite or zero. Consider a homogenous and isotropic system at an RG fixed point, where the correlation lengths diverges ($\xi \rightarrow \infty$) and therefore much larger than the short distance cutoff, which is usually the lattice spacing α . Such systems are well approximated by a continuous field theory, which has conformal symmetry.

Conformal symmetry imposes strong conditions onto the transformation properties of correlation functions. Let $\{\phi_n(\mathbf{r})\}$ be a family of operators at a fixed point with a scale invariant action, which transforms under scale transformations as

$$\phi_n(b\mathbf{r}) = b^{-\Delta_n} \phi_n(\mathbf{r}). \quad (4.1)$$

Such operators are called primary operators. It is further assumed, that the $\phi_n(\mathbf{r})$ operators are normal ordered at the fixed point $\langle \phi_n(\mathbf{r}) \rangle_* = 0$ and their correlation

functions are decaying at large distances. Conformal symmetry implies rotational, translational and scale invariance, which is only fulfilled for a power law decay

$$\langle \phi_n(\mathbf{r}_i) \phi_n(\mathbf{r}_j) \rangle_* = \frac{1}{|\mathbf{r}_i - \mathbf{r}_j|^{2\Delta_n}}, \quad (4.2)$$

where Δ_n is the scaling dimension of the operator ϕ_n . The scaling dimension can be understood as a quantum number, labeling an irreducible representation of the conformal group, similarly to an angular momentum quantum number, that corresponds to a representation of $SU(2)$. In analogy, an orthogonality condition holds

$$\langle \phi_n(\mathbf{r}_i) \phi_m(\mathbf{r}_j) \rangle_* = \frac{\delta_{\Delta_n, \Delta_m}}{|\mathbf{r}_i - \mathbf{r}_j|^{2\Delta_n}}. \quad (4.3)$$

Conformal symmetry also constraints the form of three-point functions. Belavin et al. have shown, that three-point functions of primary fields have the form

$$\langle \phi_n(\mathbf{r}_i) \phi_m(\mathbf{r}_j) \phi_l(\mathbf{r}_k) \rangle_* = \frac{C_{nmk}}{|\mathbf{r}_i - \mathbf{r}_j|^{\Delta_{nm}} |\mathbf{r}_i - \mathbf{r}_l|^{\Delta_{nl}} |\mathbf{r}_l - \mathbf{r}_j|^{\Delta_{lm}}}, \quad (4.4)$$

with

$$\Delta_{nm} = \Delta_n + \Delta_m - \Delta_k \quad (4.5)$$

$$\Delta_{nl} = \Delta_n + \Delta_l - \Delta_m \quad (4.6)$$

$$\Delta_{lm} = \Delta_l + \Delta_m - \Delta_n. \quad (4.7)$$

4.1.2 Operator Product Expansion

Consider a general multipoint function at the fixed point $\langle \dots \phi_n(\mathbf{r}_n) \phi_m(\mathbf{r}_m) \dots \rangle_*$. A family of operators is called complete, if a decomposition

$$\lim_{\mathbf{r}_i \rightarrow \mathbf{r}_j} \phi_n(\mathbf{r}_i) \phi_m(\mathbf{r}_j) = \sum_k \frac{C_{nmk}}{|\mathbf{r}_i - \mathbf{r}_j|^{\Delta_n + \Delta_m - \Delta_k}} \phi_k \left(\frac{\mathbf{r}_i + \mathbf{r}_j}{2} \right) \quad (4.8)$$

exists. Such a decomposition is called operator product expansion (OPE) and the coefficients C_{nmk} are its structure constants. It describes how two operators fuse to a new local composite operator in the vicinity of each other.

4.1.3 Perturbative renormalization group

One can use the scaling dimensions and structure constants to derive the RG equations of a system, in the vicinity of one of its fixed points. Let S be the action of a system and S^* be the fixed point action of the same system.

$$S = S^* + \delta S, \quad (4.9)$$

4.1 Perturbative renormalization group around a fixed point from operator product expansion

with

$$\delta S = \int d^D x \sum_n g_n \alpha^{\Delta_n - D} \phi_n(\mathbf{r}), \quad (4.10)$$

where g_n are dimensionless coupling constants and α is the ultra-violet (UV) cutoff. It is assumed that the perturbation operators $\phi_n(\mathbf{r})$ are primary and obey the properties, which were presented in the previous subsection. The deviation of the partition function from its value at the fixed point is given in third order perturbation theory by

$$\begin{aligned} \frac{Z}{Z_*} = & 1 + \sum_n \int \frac{d^D \mathbf{r}}{\alpha^{D-\Delta_n}} g_n \langle \phi_n(\mathbf{r}) \rangle_* + \\ & + \frac{1}{2} \sum_{n,m} \int \frac{d^D \mathbf{r}_1}{\alpha^{D-\Delta_n}} \int \frac{d^D \mathbf{r}_2}{\alpha^{D-\Delta_m}} g_n g_m \langle \phi_n(\mathbf{r}_1) \phi_m(\mathbf{r}_2) \rangle_* + \\ & + \frac{1}{6} \sum_{n,m,k} \int \frac{d^D \mathbf{r}_1}{\alpha^{D-\Delta_n}} \int \frac{d^D \mathbf{r}_2}{\alpha^{D-\Delta_m}} \int \frac{d^D \mathbf{r}_3}{\alpha^{D-\Delta_k}} g_n g_m g_k \langle \phi_n(\mathbf{r}_1) \phi_m(\mathbf{r}_2) \phi_k(\mathbf{r}_3) \rangle_* + \dots \end{aligned} \quad (4.11)$$

The partition function Z shall be fixed during an RG transformation, which consists of 1) change of UV cutoff and 2) rescaling of the dimensionless couplings. It is convenient to parametrize the change of the UV cutoff logarithmically $\alpha \rightarrow e^{\delta l} \alpha$. Rescaling of α affects the partition sum (4.11) twofold: via the denominator of the integrand and at the lower boundary of the integration region. The denominator of the integrand transforms as

$$\frac{g_n}{\alpha^{D-\Delta_n}} \rightarrow \frac{g_n}{\alpha^{D-\Delta_n} e^{(D-\Delta_n)\delta l}}, \quad (4.12)$$

which can be compensated by a change of the dimensionless couplings

$$g_n \rightarrow g_n e^{(D-\Delta_n)\delta l} \approx g_n + g_n (D - \Delta_n) \delta l. \quad (4.13)$$

Apparently, this gives the familiar one loop contribution to the RG equations

$$\frac{dg_n}{dl} = (D - \Delta_n) g_n. \quad (4.14)$$

The contribution to the RG equations from changing the lower boundary of the integrals can be evaluated using the OPE. Consider therefore the second order contribution to the partition sum. The double integral can be divided into two

subregions

$$\begin{aligned}
 & \int_{|\mathbf{r}_1 - \mathbf{r}_2| > \alpha(1+\delta l)} d^D \mathbf{r}_1 d^D \mathbf{r}_2 F(\mathbf{r}_1, \mathbf{r}_2) = \\
 & = \int_{|\mathbf{r}_1 - \mathbf{r}_2| > \alpha} d^D \mathbf{r}_1 d^D \mathbf{r}_2 F(\mathbf{r}_1, \mathbf{r}_2) - \int_{\alpha(1+\delta l) > |\mathbf{r}_1 - \mathbf{r}_2| > \alpha} d^D \mathbf{r}_1 d^D \mathbf{r}_2 F(\mathbf{r}_1, \mathbf{r}_2).
 \end{aligned} \tag{4.15}$$

The first gives simply the original contribution to Z , while the second can be expanded into an OPE

$$\begin{aligned}
 & \frac{1}{2} \sum_{n,m} \int \frac{d^D \mathbf{r}_1}{\alpha^{D-\Delta_n}} \int \frac{d^D \mathbf{r}_2}{\alpha^{D-\Delta_m}} g_n g_m \langle \phi_n(\mathbf{r}_1) \phi_m(\mathbf{r}_2) \rangle_* = \\
 & = \frac{1}{2} \sum_{n,m,k} \iint d^D \mathbf{r}_1 d^D \mathbf{r}_2 \frac{g_n g_m}{\alpha^{2D-\Delta_n-\Delta_m}} \frac{C_{nmk}}{|\mathbf{r}_1 - \mathbf{r}_2|^{\Delta_n+\Delta_m-\Delta_k}} \left\langle \phi_k \left(\frac{\mathbf{r}_1 + \mathbf{r}_2}{2} \right) \right\rangle_* = \\
 & = \frac{1}{2} \sum_{n,m,k} C_{n,m,k} g_n g_m \alpha^{\Delta_k - \Delta_n - \Delta_m + 1} \int \frac{d^D \mathbf{r}}{\alpha^{2D-\Delta_n-\Delta_m}} \langle \phi_k(\mathbf{r}) \rangle_* S_D \alpha^{D-1} \delta l = \\
 & = \frac{1}{2} \sum_{n,m,k} C_{n,m,k} g_n g_m \int \frac{d^D \mathbf{r}}{\alpha^{D-\Delta_k}} \langle \phi_k(\mathbf{r}) \rangle_* S_D \delta l,
 \end{aligned} \tag{4.16}$$

where S_D is the D -dimensional volume of the D -sphere.

From Equation (4.16) we can read off the appropriate rescaling of the couplings, which compensates for this contribution to be

$$g_k \rightarrow g_k - \frac{1}{2} S_D \sum_{n,m} C_{n,m,k} g_n g_m \delta l. \tag{4.17}$$

Apparently, this gives the one-loop contribution to the RG equations. Because only infinitesimal transformations of α are considered, the total RG flow equation is provided by the sum of the two contributions, which reads after a redefinition of the couplings $g_k \rightarrow \frac{2}{S_D} g_k$

$$\frac{dg_k}{dl} = (D - \Delta_k) g_k - \sum_{n,n} C_{n,m,k} g_n g_m. \tag{4.18}$$

4.2 Derivation of the RG equations for the helical edge state with Kondo impurities

In order to acquire a rough understanding of the properties of the system it is useful to perform a renormalization group analysis. A similar work for a discrete lattice of magnetic impurities has been done by Maciejko [24], by mapping the problem to the 2D Coulomb gas model. We will focus on the case of a continuous distribution of impurities and treat it using operator product expansion (OPE). We consider again a bosonized action of interacting helical edge electrons with magnetic impurities, where the J_z in-plane component of coupling between electrons and localized spins was eliminated by the procedure described in the last section.

$$S = \frac{1}{2\pi K} \int_{-\infty}^{\infty} dx \int_0^{\infty} d\tau \left[\frac{1}{u} (\partial_\tau \phi)^2 + u (\partial_x \phi)^2 \right] + \frac{J_\perp S}{2\pi \xi} \int_{-\infty}^{\infty} dx \int_0^{\infty} d\tau \rho(x) \left[\sqrt{1 - n_z^2(x, \tau)} e^{i\alpha(x, \tau)} e^{-i2\phi(x, \tau)} + \text{h.c.} \right] + S_{WZ}. \quad (4.19)$$

It is instructive to shift the ϕ field $\phi(x, \tau) - \frac{\alpha(x, \tau)}{2} \rightarrow \phi(x, \tau)$. The action then reads

$$S = \frac{1}{2\pi K} \int_{-\infty}^{\infty} dx \int_0^{\infty} d\tau \left[\frac{1}{u} (\partial_\tau \phi)^2 + u (\partial_x \phi)^2 \right] + \frac{1}{2\pi K} \int_{-\infty}^{\infty} dx \int_0^{\infty} d\tau \left[\frac{1}{u} (\partial_\tau \alpha)^2 + u (\partial_x \alpha)^2 \right] + \frac{J_\perp S}{\pi \xi} \int_{-\infty}^{\infty} dx \int_0^{\infty} d\tau \rho(x) \sqrt{1 - n_z^2(x, \tau)} \cos [2\phi(x, \tau)] + S_{WZ}. \quad (4.20)$$

It is further assumed, that n_z is still a slow variable. So that the model essentially reduces to a sine-gordon model, which RG equations are the well-known Kosterlitz-Thouless RG equations.

The scaling dimension d of the cosine can be derived from the two-point correlation function

$$\left\langle e^{i2\phi(x, \tau)} e^{-i2\phi(0, 0)} \right\rangle = \frac{1}{[x^2 + u^2 \tau^2]^K}, \quad (4.21)$$

so that

$$d = K. \quad (4.22)$$

The terms from the OPE, which contribute to the RG equations are

$$\lim_{x \rightarrow y} : e^{in\phi(x)} :: e^{-in\phi(y)} = \frac{1}{|x - y|^{2K}} - \frac{1}{|x - y|^{2K-2}} \frac{n^2}{2} \left[(\partial_x \phi)^2 + \frac{1}{u^2} (\partial_\tau \phi)^2 \right] \quad (4.23)$$

We can read off the OPE coefficient of interest

$$C_{n,-n,0} = \frac{n^2}{2} \quad (4.24)$$

from which one immediately arrives at the RG equations

$$\frac{dJ_{\perp}}{dl} = (2 - K)J_{\perp} \quad (4.25)$$

$$\frac{dK}{dl} = \frac{1}{2}J_{\perp}^2 K^2 \quad (4.26)$$

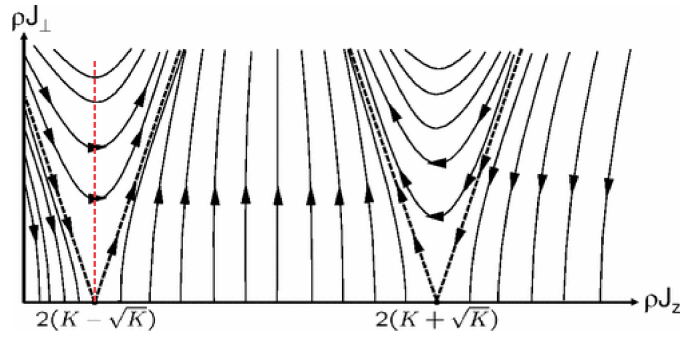


Figure 4.1: RG flow for the density of magnetic impurities embedded into a helical edge liquid (Source: [24])

4.3 Discussion of the RG equations

The picture above suggests that J_{\perp} flows to strong coupling at all $K < 2$. However, we know from the case of $K = 1$ (red line), which corresponds exactly to the work by Altshuler et al., that strong coupling does not correctly capture the physics. In the fermionic calculation the RG flow can cut by the large gap in the fermionic spectrum. So, while the RG equations are significant in the strongly attractive region, where they suggest that backscattering becomes irrelevant and perfect conductance is restored, in the region $K < 2$ the only information we can extract from them is, that we are deeply in a massive regime. To gain further insight into the physical properties of this regime we are required to construct an effective massive theory for this regime. This will be the subject of the next chapter.

Chapter 5

Effective Action for the Interacting Edge Mode of Topological Insulators with Kondo Impurities

In the last section we have argued, that in order to access the transport properties of the region $K < 2$, we need to construct an effective gapped action. We will do so self-consistently using Feynman's variational principle [12].

5.1 Construction of a variational free energy functional

The basic idea behind Feynman's variational principle is to construct a variational free energy functional from an upper bound of the true free energy and minimize it in the subspace of all variational actions. The subspace of variational actions is usually, like in our case, the space of all quadratic actions.

Let S_{ini} be the full action of our problem and S_0 an action from the subspace of variational actions. It is possible to express the free energy of the system described by S_{ini} using averages with respect to S_0 as follows

$$\begin{aligned} F &= -T \log \left(\int D\phi e^{-S_{\text{ini}}} \right) = -T \log \left(\int D\phi e^{-S_0} e^{-(S_{\text{ini}} - S_0)} \right) = \\ &= F_0 - T \log \langle e^{-(S_{\text{ini}} - S_0)} \rangle_0. \end{aligned} \quad (5.1)$$

The expression on the right hand side is exact and usually very difficult to compute. Using the convexity property of the exponential function, $\langle e^X \rangle \geq e^{\langle X \rangle}$, one can derive an upper bound for the free energy (5.1)

$$F \leq F_{\text{var}}[S_0] = F_0 + T \langle S_{\text{ini}} - S_0 \rangle_0. \quad (5.2)$$

If we have chosen an appropriate subspace of variational actions, it is possible to evaluate Equation (5.2) for every one of them. By minimizing $F_{\text{var}}[S_0]$ over the subspace of all variational actions, we arrive at an effective action, which approximates the full action S_{ini} .

5.2 Computation of the effective action for the interacting helical edge

Let us apply the procedure outlined before to our system. The full action reads

$$S = \frac{1}{2\pi K} \int_{-\infty}^{\infty} dx \int_0^{\infty} d\tau \left[\frac{1}{u} (\partial_{\tau} \phi)^2 + u (\partial_x \phi)^2 \right] + \frac{1}{2\pi K} \int_{-\infty}^{\infty} dx \int_0^{\infty} d\tau \left[\frac{1}{u} (\partial_{\tau} \alpha)^2 + u (\partial_x \alpha)^2 \right] + \frac{J_{\perp} S}{2\pi \xi} \int_{-\infty}^{\infty} dx \int_0^{\infty} d\tau \rho(x) \sqrt{1 - n_z^2(x, \tau)} \cos [2\phi(x, \tau)] + S_{WZ}. \quad (5.3)$$

As before, we will assume the fields $\alpha(x, \tau), n_z(x, \tau)$ to be constant on the characteristic scale of the bosonic field $\phi(x, \tau)$, so we will disregard the terms which depend only on them for a moment and focus on deriving an effective action for the bosonic sector gapped due to backscattering off magnetic impurities

$$S_{\text{ini}} = \frac{1}{2\pi K} \int_{-\infty}^{\infty} dx \int_0^{\infty} d\tau \left[\frac{1}{u} (\partial_{\tau} \phi)^2 + u (\partial_x \phi)^2 \right] - \frac{J_{\perp} S}{2\pi \xi} \int_{-\infty}^{\infty} dx \int_0^{\infty} d\tau \rho(x) \sqrt{1 - n_z^2(x, \tau)} \cos [2\phi(x, \tau)]. \quad (5.4)$$

The variational quadratic action has the general form

$$S_0 = \frac{1}{2\beta L} \sum_{\mathbf{q}} G^{-1}(\mathbf{q}) \phi^*(\mathbf{q}) \phi(\mathbf{q}). \quad (5.5)$$

By plugging 5.4 and 5.5 into Equation (5.2) on the previous page, we can compute the variational free energy dependeng on $G(\mathbf{q})$

$$F_{\text{var}} = -\frac{T}{2} \sum_{\mathbf{q}} G(\mathbf{q}) + \frac{T}{2\pi u K} \sum_{\mathbf{q}} [\omega^2 + u^2 k^2] G(\mathbf{q}) - \frac{J_{\perp} S N \sqrt{1 - n_z^2}}{2\pi \xi} e^{-\frac{2}{\beta L} \sum_{\mathbf{q}} G(\mathbf{q})}. \quad (5.6)$$

The stationarity condition $\frac{\delta F_{\text{var}}}{\delta G(\mathbf{q})} \stackrel{!}{=} 0$ implies a self-consistent equation for the Green's function $G(\mathbf{q})$

$$G^{-1}(\mathbf{q}) = \frac{1}{\pi u K} [\omega^2 + u^2 k^2] + \frac{2J_{\perp} S \sqrt{1 - n_z^2} \bar{\rho}}{\pi \xi} e^{-\frac{2}{\beta L} \sum_{\mathbf{q}} G(\mathbf{q})}, \quad (5.7)$$

which can be solved with the ansatz

$$G^{-1}(\mathbf{q}) = \frac{1}{\pi u K} [\omega^2 + u^2 k^2 + \Delta^2]. \quad (5.8)$$

The gap can be computed by plugging the ansatz 5.8 into 5.7, which leads to

$$\frac{\Delta^2}{\pi u K} = \frac{2J_{\perp} S \sqrt{1 - n_z^2 \bar{\rho}}}{\pi \xi} e^{-K \log(\frac{D}{\Delta})}, \quad (5.9)$$

which can be solved for Δ

$$\Delta = D \left(\frac{2J_{\perp} S \sqrt{1 - n_z^2 \bar{\rho}} K}{D} \right)^{\frac{1}{2-K}}. \quad (5.10)$$

5.3 Properties of the effective action

5.3.1 Form of the gap

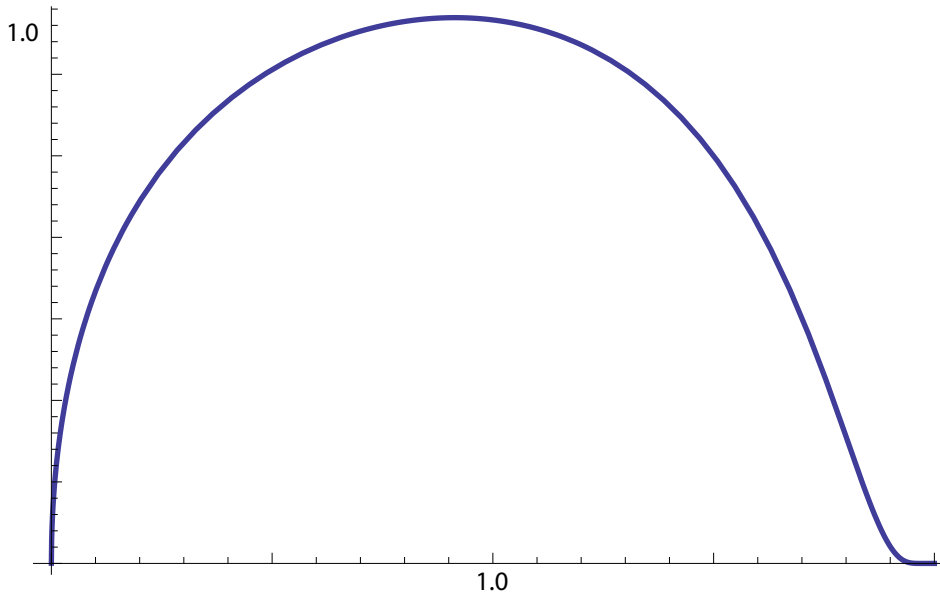


Figure 5.1: Plot of the gap for $0 < K < 2$

The qualitative dependence of the gap on the Luttinger parameter is depicted in Figure 5.1. It is maximal for moderate attractive or repulsive interaction strengths. For strongly attractive interactions backscattering becomes irrelevant, so that the gap goes to zero. Near $K = 0$ backscattering is suppressed by the onset of Wigner crystallization, so that the gap becomes zero as well. The gap naturally also goes to zero, if the density of the impurities is reduced.

5.3.2 Free energy

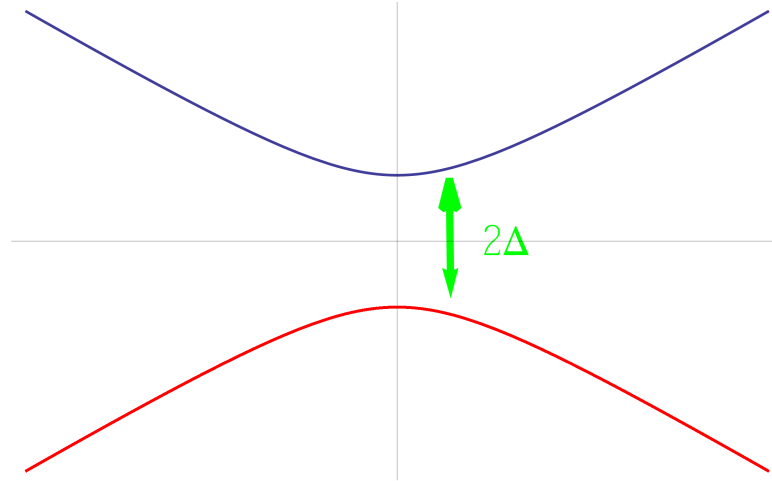


Figure 5.2: Spectrum of the gapped bosons, the lower branch of the spectrum is unphysical

It is well known [22], that in bosonic systems the chemical potential must lie at or below the lowest occupied energy level. Hence, a gapped bosonic system at zero temperature has free energy zero. If one looks at our effective bosonic action, one is tempted to believe, that this doesn't hold in our case. The chemical potential is at zero, while the dispersion relation $\omega = \pm\sqrt{u^2k^2 + \Delta^2}$ is unbound from below. Therefore we need to subtract the free energy that comes from the unphysical occupied states below the chemical potential, in order to be capable of properly extracting physical quantities.

Chapter 6

Physics from the effective action

6.1 Transport properties of an helical edge state coupled to magnetic impurities from bosonization

6.1.1 Isotropically in-plane coupled impurities

In the same spirit as in Altshuler et al [2]. for the case of non-interacting helical edge states, we want to derive an effective action for $\alpha(x, \tau)$. Hence, we start with the effective gapped gaussian action derived in the previous section together with the terms, which describe the degrees of freedom of the impurity, which were disregarded in equation (5.5) on page 32 and an additional source term $h(x, \tau)$, which initially coupled to the density $\partial_x \phi(x, \tau)$ and after the shift (equation (4.20) on page 29) couples both to the $\partial_x \phi(x, \tau)$ and $\partial_x \alpha(x, \tau)$

$$S = S_{\text{eff}} + \int_{-\infty}^{\infty} dx \int_0^{\infty} d\tau h(x, \tau) \partial_x \phi(x, \tau) + \frac{1}{2\pi K} \int_{-\infty}^{\infty} dx \int_0^{\infty} d\tau \left[\frac{1}{u} (\partial_\tau \alpha)^2 + u (\partial_x \alpha)^2 \right] + h(x, \tau) \partial_x \alpha(x, \tau) + S_{\text{WZ}}. \quad (6.1)$$

Following the ideology from chapter 2, we want to derive the contribution to the action from quadratic fluctuations of the out-of-plane component of the impurity spins $n_z(x, \tau)$. In the previous section, we briefly outlined, that we need to subtract contributions to the free energy from an ill branch of the bosonic spectrum, that lies below the chemical potential. Fluctuations of n_z lead to fluctuations of the magnitude of the gap and so for a change in the energy, which is subtracted. It is this contribution, where we can extract the contribution of fluctuations of n_z to the action from. The precise technicalities of the procedure are presented in the appendix. The effective term has the same form as for the non-interacting helical edge, except that the bosonic gap from equation (5.10) on page 33 is substituted

in place of the fermionic gap

$$S_{n_z} = \int dx d\tau \Delta^2(x) \log \left(\frac{D}{\Delta(x)} \right) n_z^2. \quad (6.2)$$

By integrating out $n_z(x, \tau)$ we get the effective action for $\alpha(x, \tau)$:

$$S_{\text{eff}} = \frac{1}{2\pi u_\alpha K_\alpha} \int dx d\tau \left[(\partial_\tau \alpha)^2 + u^2 (\partial_x \alpha)^2 \right] - \frac{1}{2\pi} \int dx d\tau h(x, \tau) \partial_x \alpha, \quad (6.3)$$

which has, as expected, the form of a Tomonaga-Luttinger action with

$$K_\alpha = K \frac{u_\alpha}{u} \quad u_\alpha = u \sqrt{\frac{4\Delta^2 \log \left(\frac{D}{\Delta} \right)}{uK\bar{\rho}^2 + 4\Delta^2 \log \left(\frac{D}{\Delta} \right)}} \quad (6.4)$$

We have therefore ideal conductance with Drude weight $\frac{u^2}{v_F^2}$.

6.1.2 Anisotropically in-plane coupled impurities

Analogously to the non-interacting case, adding a random anisotropy to the boson-impurity coupling will add a disorder term to S_{eff} . To show this, we start with action (4.19) and add a random anisotropy term to the coupling between electrons and bosons

$$S_{\text{ani}} = S + \frac{J_\perp S}{2\pi\xi} \int_{-\infty}^{\infty} dx \int_0^{\infty} d\tau \rho(x) \left[\sqrt{1 - n_z^2(x, \tau)} \epsilon(x) e^{i\alpha(x, \tau)} e^{i2\phi(x, \tau)} + \text{h.c.} \right]. \quad (6.5)$$

As before, we shift the ϕ field $\phi(x, \tau) - \frac{\alpha(x, \tau)}{2} \rightarrow \phi(x, \tau)$

$$S_{\text{ani}} = S + \frac{J_\perp S}{2\pi\xi} \int_{-\infty}^{\infty} dx \int_0^{\infty} d\tau \rho(x) \left[\sqrt{1 - n_z^2(x, \tau)} \epsilon(x) e^{i2\alpha(x, \tau)} e^{i2\phi(x, \tau)} + \text{h.c.} \right] \quad (6.6)$$

Following the steps from previous section, we arrive at a modified expression for the gap, where we neglect terms, that are higher order in n_z and ϵ .

$$\Delta = D \left(\frac{2J_\perp S \sqrt{1 - n_z^2} [1 + \epsilon(x) e^{i2\alpha(x, \tau)} + \epsilon^*(x) e^{-i2\alpha(x, \tau)}] \bar{\rho} K}{D} \right)^{\frac{1}{2-K}} \quad (6.7)$$

The derivation of the contributions of n_z and the anisotropy to the action is outlined in the appendix. Compared to the isotropic case, anisotropy gives here, exactly as in the non-interacting fermionic case, rise to an additional term of the form

$$S_{\text{ani}} = S_{\text{eff}} + \int dx d\tau \mathcal{E}^2(x) \cos [2\alpha(x, \tau) - \gamma(x)]. \quad (6.8)$$

Such action describes a disorder Luttinger liquid. Its physics has been discussed using a renormalization group approach by Giamarchi and Schulz. A short review of their work is provided in the appendix. For $K_\alpha < \frac{3}{2}$ disorder induces Anderson localization, so that the dc conductance goes down to zero. At $K_\alpha = \frac{3}{2}$ the system undergoes a phase transition to a conductor.

6.2 Helical edge states at attractive interaction with magnetic impurities

The scenario described in the previous section holds for small attractive interactions, $1 < K < 2$. As long as backscattering of the bosons by the Kondo impurities and the anisotropy in their coupling is relevant, the system stays an insulator.

As already outlined in the discussion of the RG flow of the system, the picture drastically changes for $K > 2$. In this region backscattering is irrelevant, so that the system becomes an ideal helical edge state.

The analysis from the previous section relies heavily on the fact that one is deep in the massive phase, where the spins are ordered and we have separate characteristic lengthscales for the fields describing bosons and spins. This does not hold for the region $K \lesssim 2$, so that our bold analysis is not capable of capturing the essential features of that region. However, as we know that we are in an insulating phase for $K = 1$ and in an ideal conducting helical edge state for $K > 2$, we can conclude, that there must be an insulator-conductor phase transition inbetween.

6.3 Helical edge states at repulsive interaction with magnetic impurities

For weak interacting helical edge states $K \lesssim 1$ we have a gap that is large compared to the Kondo temperature, so that all of our arguments from the first section hold true and we have an Anderson insulator, due to random anisotropy. For strong interactions ($K \rightarrow 0$) and low density ($\bar{\rho} \rightarrow 0$) the gap goes to zero. The range of correlations between magnetic impurities becomes smaller until single impurity physics becomes important [38, 8]. As was discussed in Chapter 2, at zero temperature, single Kondo impurities become screened and decouple from the helical liquid. The characteristic energy scale for this process is provided by the Kondo temperature

$$T_K = D \left(\frac{J_\perp}{1-K} \right)^{\frac{1}{1-K}}. \quad (6.9)$$

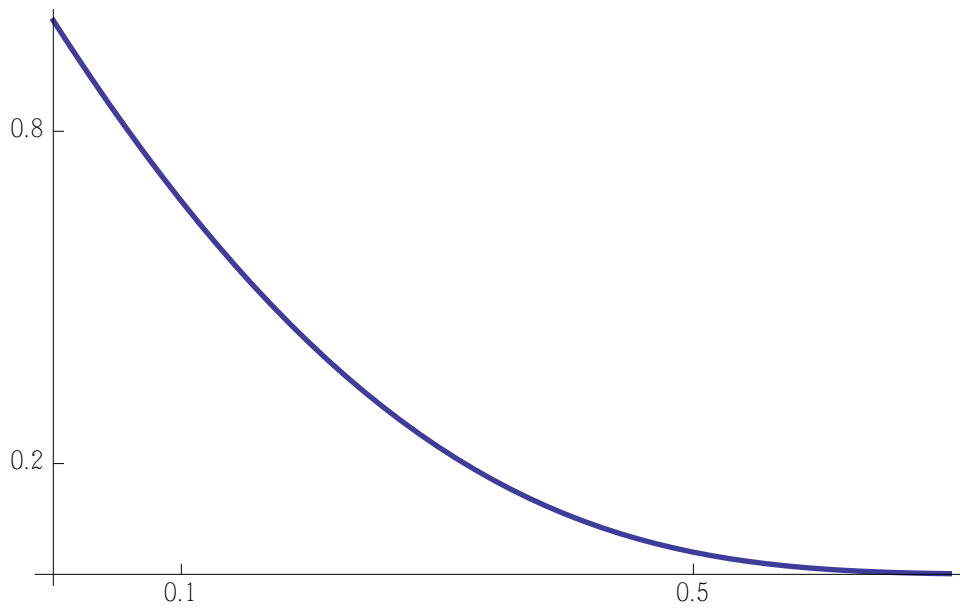


Figure 6.1: Plot of $\frac{T_K}{100D}$ for $J_\perp = 0.01$ (limit of $1 - K \gg J_\perp$)

As opposed to the gap Δ , the Kondo temperature grows as $K \rightarrow 0$. In the region, where $T_K \gg \Delta$ Kondo screening dominates the physics of the edge state. When all impurities are screened and decoupled from the helical edge, it becomes again an ideal conductor. Thus, the system undergoes an insulator-conductor transition.

6.4 Phase diagram of helical edge states with magnetic impurities

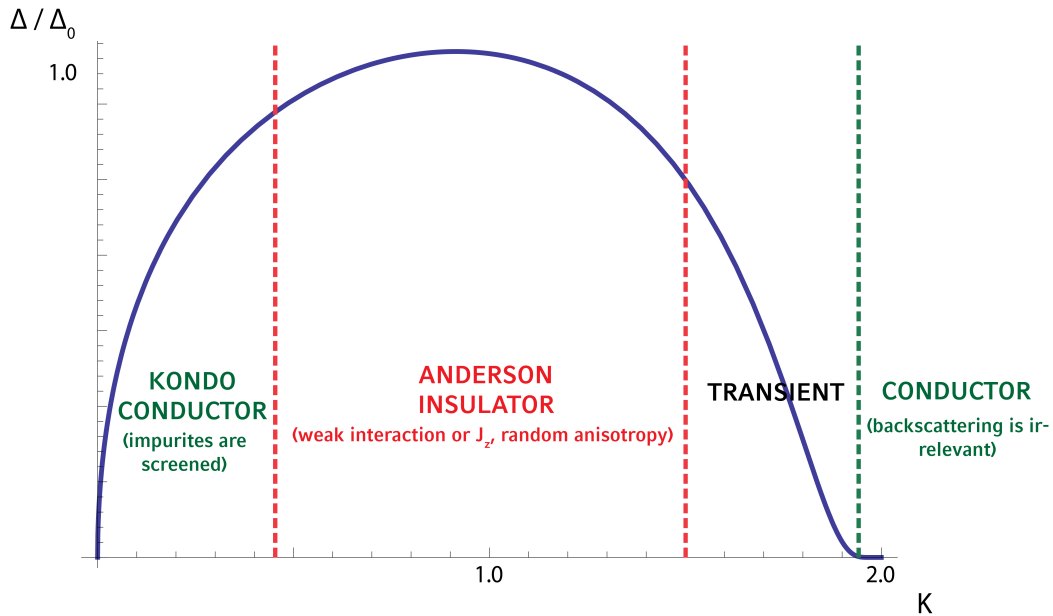


Figure 6.2: Phase diagram of the helical edge state with Kondo impurities

The discussion above is summarized in the diagram 6.2. For strong repulsive interactions and low density of impurities, the gap goes to zero and the Kondo impurities become screened. Screened impurities decouple from the edge, which thusly becomes conducting.

When interactions are reduced, magnetic ordering of the spins prevents the impurity from being screened. Then, if the coupling between the edge and the impurity is in-plane and randomly anisotropic, the edge state becomes localized. The localized state is stable for small-to-intermediate repulsive or attractive interactions, until backscattering becomes irrelevant at strongly attractive interaction strengths, turning the edge again ideally conducting.

Chapter 7

Conclusion, Open questions and Outlook

7.1 Conclusion

We have discussed the properties of interacting edge states of quantum spin Hall insulators coupled to magnetic impurities. The out-of-plane coupling between impurities and edge plays an important role, as it was shown to be equivalent to altered interactions inside the edge. From Feynman's variational principle, an effective gapped gaussian action for the system was constructed. A rich phase diagram was uncovered using the effective action. For high impurity densities and weak-to-intermediate interactions, the system is an Anderson insulator, like in the non-interacting case, which was considered by Altshuler et al., previously. At low density and strong repulsive interactions the system undergoes a insulator-conductor phase transition due to the onset of Kondo screening. At strong attractive interactions, the system undergoes a insulator-conductor phase transition as well, since backscattering becomes irrelevant there.

7.2 Open questions

7.2.1 Critical properties of the transition region

While our approach is sufficient to argue for the presence of phase transitions, it does not capture accurately the critical properties in the transition region. In the repulsive region, we can argue, that at some point Kondo screening dominates over the ordering of the spins, but neither the exact value of K nor the type of phase transition can be deduced from that reasoning. Similarly for attractive interactions, we could naively expect a phase transition at $K = 2$, however, as the gap decreases, they do not have a clear separation of lengthscales, deeming our derivation and the effective action for $\alpha(x, \tau)$ inapplicable.

7.2.2 \mathbb{Z}_2 Invariant

While our discussion implies a series of phase transitions, we have so far not touched at all the question of how this should be understood in terms of bulk-boundary correspondence and the \mathbb{Z}_2 invariant. Our predictions are supported by purely one-dimensional calculations, although we use the fact, that the underlying physical object is two-dimensional, when we claim, that the screened Kondo impurity decouples from the edge liquid, instead of blocking any transport through it, as would be the case in a truly one-dimensional Luttinger liquid. In fact, it was shown by Wu et al., that a helical edge state can not exist as a one-dimensional object. Thus, in order to understand, whether our results imply topological phase transitions, it is indispensable to perform a calculation of the \mathbb{Z}_2 invariant with a two-dimensional Hamiltonian of a quantum spin Hall insulator.

Appendix A

Bosonization of an helical edge state

A.1 Construction of a bosonic representation of the Hamiltonian

The edge state of a quantum spin Hall insulator is effectively one dimensional and consists of two species of counterpropagating Dirac fermions [29]

$$H = -iv_f \int dx [\bar{\Psi}_R \partial_x \Psi_R - \bar{\Psi}_L \partial_x \Psi_L]. \quad (\text{A.1})$$

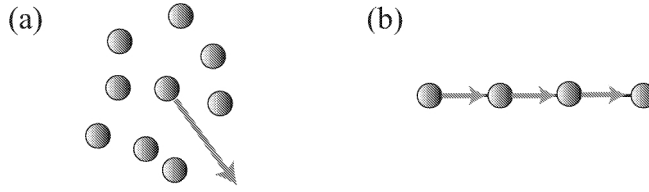


Figure A.1: Comparison between single particle excitations in (a) higher dimensions and (b) one dimension (Source: [12])

It is a special feature of one dimensional systems, that unlike in higher dimensions, it is not possible to excite a single particle-hole excitation in them, but every excitation is a collective density fluctuation

$$\rho^\dagger(q) = \sum_k \psi_{k+q}^\dagger \psi_k. \quad (\text{A.2})$$

Therefore, one can expect, that it is possible to represent the Hamiltonian in terms of such density fluctuations. For the construction, we follow the book by Giamarchi [12]. One is interested in doing so, because density-density interactions

$$H_{\text{int}} = \frac{1}{2L} \sum_q V(q) \rho^\dagger(q) \rho(q) \quad (\text{A.3})$$

are quadratic in these operators, so that the problem of interacting fermions becomes exactly solvable.

Since one would like to derive a representation of the Hamiltonian in terms of excitations from the ground state and to avoid divergences, which come from the unboundness of the spectrum of Dirac fermions from below, one considers normal ordered operators. Define

$$:\rho_r(x): = :\psi_r^\dagger(x)\psi_r(x): = \frac{1}{L} \sum_p :\rho_r(p): e^{ipx}, \quad (\text{A.4})$$

the density of right/left ($r = R/L$) movers, with the Fourier component

$$:\rho_r(p): = \begin{cases} \sum_k \psi_{r,k+p}^\dagger \psi_{r,k}, & p \neq 0 \\ N_r, & p = 0 \end{cases}, \quad (\text{A.5})$$

where N_r is defined as

$$N_r = \sum_k \left[\psi_{r,k}^\dagger \psi_{r,k} - \langle 0 | \psi_{r,k}^\dagger \psi_{r,k} | 0 \rangle \right]. \quad (\text{A.6})$$

Using the commutation relations of the fermions, it is possible to derive commutation relations for the density fluctuation operators. Densities of different species commute

$$\left[\rho_R^\dagger(p), \rho_L^\dagger(p') \right] = 0. \quad (\text{A.7})$$

For identical species one has to take properly care of subtraction of divergences, in order to arrive at the correct result

$$\begin{aligned} \left[\rho_r^\dagger(p), \rho_r^\dagger(-p') \right] &= \sum_{k,k'} \left[\psi_{r,k+p}^\dagger \psi_{r,k'}, \psi_{r,k'-p'}^\dagger \psi_{r,k'} \right] = \\ &= \sum_{k,k'} \left(\psi_{r,k+p}^\dagger \psi_{r,k'} \delta_{k,k'-p'} - \psi_{r,k'-p'}^\dagger \psi_{r,k} \delta_{k',k+p} \right) = \\ &= \sum_k \left(\psi_{r,k+p}^\dagger \psi_{r,k+p'} - \psi_{r,k+p-p'}^\dagger \psi_{r,k} \right) = \\ &= \underbrace{\sum_k \left(:\psi_{r,k+p}^\dagger \psi_{r,k+p'}: - :\psi_{r,k+p-p'}^\dagger \psi_{r,k}: \right)}_{\sum_k :\psi_{r,k+p}^\dagger \psi_{r,k+p'}: - \sum_{k'} :\psi_{r,k'+p}^\dagger \psi_{r,k'+p'}: = 0} + \end{aligned} \quad (\text{A.8})$$

$$\begin{aligned} &+ \sum_k \left(\langle 0 | \psi_{r,k+p}^\dagger \psi_{r,k+p'} | 0 \rangle - \langle 0 | \psi_{r,k+p-p'}^\dagger \psi_{r,k} | 0 \rangle \right) = \\ &= \sum_k \left(\langle 0 | \psi_{r,k+p}^\dagger \psi_{r,k+p'} | 0 \rangle - \langle 0 | \psi_{r,k+p-p'}^\dagger \psi_{r,k} | 0 \rangle \right). \end{aligned} \quad (\text{A.9})$$

A.1 Construction of a bosonic representation of the Hamiltonian

Equation (A.9) on the facing page can be evaluated for given single particle creation- and annihilation operators. In the simple case of periodic boundary conditions

$$\left[\rho_r^\dagger(p), \rho_r^\dagger(-p') \right] = -\delta_{r,r'} \delta_{p,p'} \frac{rpL}{2\pi}. \quad (\text{A.10})$$

Up to a normalization factor, this is the commutation relation for a species of bosonic particles ($p > 0$)

$$b_p^\dagger = \sqrt{\frac{2\pi}{L|p|}} \sum_r \theta(rp) \rho_r^\dagger(p) \quad (\text{A.11})$$

$$b_p = \sqrt{\frac{2\pi}{L|p|}} \sum_r \theta(rp) \rho_r^\dagger(-p), \quad (\text{A.12})$$

where the Heaveside functions $\theta(rp)$ ensure, that left moving excitations have negative momentum and right moving excitations have positive momentum.

Assume, that the b operators generate a complete basis of all possible excitations, so that it is also possible to represent the Hamiltonian $H = v_F \sum_{r,q} r q \psi_{r,q}^\dagger \psi_{r,q}$ with them. Consider therefore the commutator ($p \neq 0$)

$$\begin{aligned} [b_p, H] &= \sqrt{\frac{2\pi}{L|p|}} \sum_{r,r',k,q} v_F q \theta(rp) \left[\rho_r^\dagger(-p), \psi_{r',q}^\dagger \psi_{r',q} \right] = \\ &= \sqrt{\frac{2\pi}{L|p|}} \sum_{r,r',q,k} v_F q \theta(rp) \left[\psi_{r,k-p}^\dagger \psi_{r,k}, \psi_{r',q}^\dagger \psi_{r',q} \right] = \\ &= \sqrt{\frac{2\pi}{L|p|}} \sum_{r,r',q,k} v_F q \theta(rp) \left(\psi_{r,k-p}^\dagger \psi_{r,q} \delta_{r,r'} \delta_{k,q} - \psi_{r,q}^\dagger \psi_{r,k} \delta_{r,r'} \delta_{k-p,q} \right) = \\ &= v_F p \sqrt{\frac{2\pi}{L|p|}} \sum_{r,k} \theta(rp) \psi_{r,k-p}^\dagger \psi_{r,k} = v_F p \sqrt{\frac{2\pi}{L|p|}} \sum_r \theta(rp) \rho_r^\dagger(-p) = \\ &= v_F p b_p. \end{aligned} \quad (\text{A.13})$$

The commutator between the Hamiltonian and a bosonic creation operator can be derived analogously.

Apparently, a Hamiltonian, that would suffice the commutation relation (A.13) has the form

$$H = \frac{\pi v_F}{L} \sum_r N_r^2 + \sum_{p \neq 0} v_F |p| b_p^\dagger b_p, \quad (\text{A.14})$$

where the first term on the latter side corresponds to the $p = 0$ contribution to the Hamiltonian.

A.2 Bosonic representation of the single-particle operators

In order to express every fermionic process through bosonic operators, one would like to find a bosonic representation of the single particle creation- and annihilation operators. Similarly to the derivation of the Hamiltonian one can compute the commutator

$$\left[\rho_r^\dagger(p), \psi_r(x) \right] = \frac{1}{L} \sum_{k,q} e^{iqx} \left[\psi_{r,k+p}^\dagger \psi_{r,k}, \psi_{r,q} \right] = -e^{ipx} \psi_r(x).$$

An operator that fulfills this commutation relation is given by

$$\psi_r(x) = U_r e^{\sum_p \frac{2\pi r}{pL} e^{ipx} \rho_r^\dagger(-p)}, \quad (\text{A.15})$$

where U_r is a so called Klein factor. Klein factors are needed, because bosonic excitation, which correspond to density fluctuations, are charge neutral, while the creation or annihilation of a fermion increases or reduces the total charge in the system. Therefore, to make the mapping between the bosonic and the fermionic basis a rigorous identity on the operator level, one needs to introduce such additional operators.

A.3 Chiral fields $\phi(x)$ and $\theta(x)$

Instead of using the bosonic operators, it is often convenient for computations a representation in terms of chiral fields $\phi(x)$ and $\theta(x)$. They are defined as

$$\phi(x) = -\pi(N_R + N_L) \frac{x}{L} - \frac{i\pi}{L} \sum_{p \neq 0} \sqrt{\frac{L|p|}{2\pi}} \frac{1}{p} \exp\left(-\frac{1}{2}\chi|p| - ipx\right) (b_p^\dagger + b_{-p}) \quad (\text{A.16})$$

$$\theta(x) = \pi(N_R - N_L) \frac{x}{L} + \frac{i\pi}{L} \sum_{p \neq 0} \sqrt{\frac{L|p|}{2\pi}} \frac{1}{|p|} \exp\left(-\frac{1}{2}\chi|p| - ipx\right) (b_p^\dagger - b_{-p}) \quad (\text{A.17})$$

where χ is a short-distance cutoff, which in the case of an edge state of a quantum spin Hall insulator, usually taken to be the penetration depth into the bulk of the material.

In the following, all quantities are understood to be evaluated in the thermodynamic limit $L \rightarrow \infty$. Using the commutation relations of the bosons, one gets the

commutation relations for the chiral fields

$$[\phi(x), \theta(y)] = i\pi \text{sgn}(x - y) \quad (\text{A.18})$$

$$\Rightarrow \left[\phi(x), \frac{1}{\pi} \nabla \theta(y) \right] = i\delta(x - y), \quad (\text{A.19})$$

$$(\text{A.20})$$

the latter has the form of a canonical comutation relation, so we can define the conjugate momentum to the field $\phi(x)$

$$\Pi(x) = \frac{1}{\pi} \nabla \theta(x). \quad (\text{A.21})$$

From Equation (A.17) on the preceding page one can give $\Pi(x)$ a physical meaning:

$$\Pi(x) = \rho_R(x) - \rho_L(x), \quad (\text{A.22})$$

which is in the case of the helical edge, where right movers are spin-up particles and left movers are spin-down particles a spin density. Similarly equation (A.16) on the facing page indicates that

$$\frac{1}{\pi} \nabla \phi(x) = \rho_R(x) + \rho_L(x), \quad (\text{A.23})$$

which is the charge density of the edge state.

Finally, the Hamiltonian and the single-particle operators can be rewritten in terms of the chiral fields

$$H = \frac{v_F}{2\pi} \int dx \left[(\pi \Pi(x))^2 + (\phi(x))^2 \right] \quad (\text{A.24})$$

and

$$\psi_r(x) = \frac{u_r}{\sqrt{2\pi\chi}} e^{irk_F x} e^{-i[r\phi(x) - \theta(x)]} \quad (\text{A.25})$$

A.4 Bosonization of an interacting helical edge state

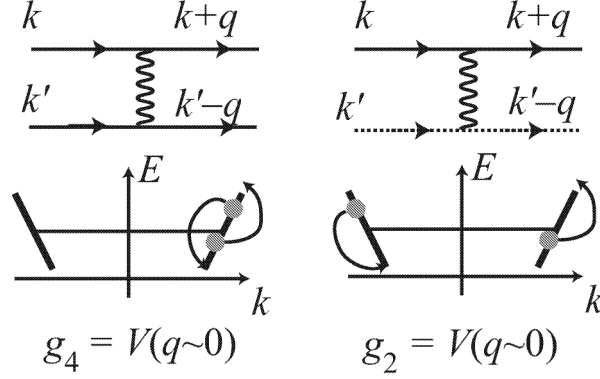


Figure A.2: Possible interaction processes in an helical edge liquid

As mentioned above, the usefulness of the bosonization procedure comes from the fact, that we can exactly the problem of one dimensional interacting fermions with it. The interaction is assumed to be short ranged. All possible interaction processes are illustrated in Figure A.2. The helical structure of the edge state only allows forward scattering, of which there are two types. Forward scattering of particles with equal chirality is described by the coupling strength g_4 . It can be cast in terms of the chiral fields using equations (A.22) and (A.23):

$$\begin{aligned} & \frac{g_4}{2} \sum_r \psi_r^\dagger(x) \psi_r(x) \sum_r \psi_r^\dagger(x) \psi_r(x) = \frac{g_4}{2} \sum_r \rho_r(x) \rho_r(x) = \\ & = \frac{g_4}{8\pi^2} \sum_r (\nabla\phi(x) - r\nabla\theta(x))^2 = \frac{g_4}{8\pi^2} [(\nabla\phi(x))^2 + (\nabla\theta(x))^2]. \end{aligned} \quad (\text{A.26})$$

Moreover, we can have forward scattering between particles of opposite chirality. That process is characterized by the g_2 coupling. Similarly to g_4 it can be rewritten in bosonic form

$$\begin{aligned} g_2 \psi_R^\dagger(x) \psi_R(x) \psi_L^\dagger(x) \psi_L(x) &= g_2 \rho_R(x) \rho_L(x) = \\ &= \frac{g_2}{4\pi^2} [(\nabla\phi(x))^2 - (\nabla\theta(x))^2]. \end{aligned} \quad (\text{A.27})$$

Eventually, one can sum the kinetic part (A.24) and the two interaction parts (A.26) and (A.27) to form a generic Hamiltonian of an interacting helical edge

$$H = \frac{1}{2\pi} \int dx \left[uK (\pi\Pi(x))^2 + \frac{u}{K} (\nabla\phi(x))^2 \right], \quad (\text{A.28})$$

where the effective constants u and K

$$u = v_F \left[\left(1 + \frac{g_4}{2\pi v_F} \right)^2 - \left(\frac{g_2}{2\pi v_F} \right)^2 \right] \quad (\text{A.29})$$

$$K = \sqrt{\frac{1 + \frac{g_4}{2\pi v_F} - \frac{g_2}{2\pi v_F}}{1 + \frac{g_4}{2\pi v_F} + \frac{g_2}{2\pi v_F}}} \quad (\text{A.30})$$

were introduced. u has the units of a velocity and can be understood as the velocity of the bosonic excitations. K is dimensionless and can in general be understood as a measure of interaction strength. $K > 1$ corresponds to systems of attractively interacting fermions, while $K < 1$ characterize phases of repulsive fermions.

Appendix B

Giamarchi-Schulz renormalization group

The problem of disordered interacting electrons in one dimension is described by the Hamiltonian [13]

$$H = H_0 + H_{\text{int}} + H_{\text{dis}}, \quad (\text{B.1})$$

where $H_0 + H_{\text{int}}$ is the Hamiltonian of interacting fermions and

$$H_{\text{dis}} = \int dx \eta(x) \left[\tilde{\psi}_R^\dagger(x) \tilde{\psi}_R(x) + \tilde{\psi}_L^\dagger(x) + \tilde{\psi}_L^\dagger(x) \right] + \quad (\text{B.2})$$

$$+ \int dx \xi(x) \left[\tilde{\psi}_R^\dagger(x) \tilde{\psi}_L(x) + \tilde{\psi}_L^\dagger(x) + \tilde{\psi}_R^\dagger(x) \right], \quad (\text{B.3})$$

where $\eta(x)$ and $\xi(x)$ are random forward- and backscattering potentials obeying gaussian statistics

$$\overline{\eta(x)\eta(x')} = D\delta(x - x') \quad (\text{B.4})$$

$$\overline{\eta(x)\xi(x')} = 0 \quad (\text{B.5})$$

$$\overline{\xi(x)\xi^*(x')} = D\delta(x - x') \quad (\text{B.6})$$

$$\overline{\xi(x)\xi(x')} = D\delta(x - x'). \quad (\text{B.7})$$

This problem was discussed using a bosonization and renormalization group approach by Giamarchi and Schulz [13, 12]. As outlined before, bosonization allows to treat interactions in this problem exactly. Disorder is then added as a perturbation, so that the total bosonized Hamiltonian reads

$$H = H_{\text{TL}} + H_{\text{dis}} \quad (\text{B.8})$$

$$H_{\text{TL}} = \frac{1}{2\pi} \int dx \left[uK (\pi\Pi(x))^2 + \frac{u}{K} (\nabla\phi(x))^2 \right] \quad (\text{B.9})$$

$$H_{\text{dis}} = - \int dx \eta(x) \frac{\nabla\phi}{\pi} + \frac{1}{2\pi\alpha} \int dx \left[\xi^*(x) e^{i2\phi(x)} + \text{h.c.} \right] \quad (\text{B.10})$$

Forward scattering can be absorbed into a shift of the ϕ field

$$\phi \rightarrow \tilde{\phi}(x) = \phi - \frac{K}{u} \int^x dy \eta(y) \quad (\text{B.11})$$

and therefore does not affect the conductivity, because current-current correlation functions are proportional to correlators of θ . The additional phase in the backscattering change does not change the statistics of the random backscattering and can be included in a redefinition of $\xi(x)$:

$$\xi(x) \rightarrow \tilde{\xi}(x) = \xi(x) e^{-i \frac{2K}{u} \int^x dy \eta(y)}. \quad (\text{B.12})$$

Hence, only the backscattering part of the disorder terms is relevant for conductance properties of the system.

When expectation value of observables are computed, one has to average over the field configurations for a given realization of disorder V

$$\langle O \rangle_V = \frac{\int D\phi O(\phi) e^{-S_V(\phi)}}{\int D\phi e^{-S_V(\phi)}} \quad (\text{B.13})$$

and over all possible realizations of the disorder

$$\overline{\langle O \rangle} = \frac{\int DV p(V) \langle O \rangle_V}{\int DV p(V)}. \quad (\text{B.14})$$

In practise it is more reasonable to perform the average over disorder before the ensemble average, so that translational symmetries of the system are restored, which simplifies the calculations. Averaging over the gaussian disorder distribution would be simple, if only the numerator would be dependent on the disorder configuration. The denominator can be transformed into a numerator turn using the replica trick. The replica trick relies on the limit

$$\frac{1}{\int D\phi e^{-S_V(\phi)}} = \lim_{n \rightarrow 0} \left[\int D\phi e^{-S_V(\phi)} \right]^{n-1}. \quad (\text{B.15})$$

Hence, one can replace the denominator by a set of replica fields and take the limit of zero replica fields at the end after the disorder averaging

$$\langle O \rangle_V = \lim_{n \rightarrow 0} \int D\phi_1 D\phi_2 \dots D\phi_n O(\phi_1) e^{-\sum_{a=1}^n S_V(\phi_a)}. \quad (\text{B.16})$$

The disorder averaged quantity reads then

$$\overline{\langle O \rangle} = \lim_{n \rightarrow 0} \int D\phi_1 D\phi_2 \dots D\phi_n O(\phi_1) e^{-S_{\text{eff}}(\phi_1, \dots, \phi_n)}, \quad (\text{B.17})$$

with an effective disorder averaged action $S_{\text{eff}}(\phi_1, \dots, \phi_n)$, where the replica fields are in general coupled with each other.

For the disordered Luttinger liquid the replicated effective action has the form

$$S_{\text{eff}} = \sum_{a=1}^n S_{\text{TL}}^a - \frac{D}{(2\pi\alpha)^2} \sum_{a=1, b=1}^n \int dx d\tau d\tau' \cos(\phi^a(x, \tau) - \phi^b(x, \tau')). \quad (\text{B.18})$$

The RG equations can be derived in a similar fashion as was outlined in chapter 4. On the tree level the flow equation for the disorder strength is

$$\frac{d\tilde{D}}{dl} = (3 - 2K)\tilde{D}, \quad (\text{B.19})$$

where $\tilde{D} = \frac{2D\alpha}{\pi u^2}$ is the unitless disorder strength.

For $K < \frac{3}{2}$ disorder is relevant and corresponds to an Anderson insulating phase [1]. When K goes above $K = \frac{3}{2}$ the disorder becomes irrelevant and the Luttinger liquid is restored. For the Anderson localized phase one can estimate the localization length as the lengthscale at which D becomes of order one. Integrating the flow equations till the localization length and then solving for it gives

$$\xi_{\text{loc}} = \alpha \left(\frac{1}{\tilde{D}} \right)^{\frac{1}{3-2K}}. \quad (\text{B.20})$$

Appendix C

Free energy of the fluctuations of n_z and $\epsilon(\chi)$ from shift of vacuum energies

We consider a gapped bosonic system, as the one corresponding to the effective action derived in chapter 5. The dispersion relation has the ill form

$$\omega = \pm \sqrt{u^2 k^2 + \Delta^2}, \quad (\text{C.1})$$

which is unphysical since it allows states below the chemical potential. Therefore we need to subtract the unphysical lower branch from all of our calculations.

In our problem, the gap has the form given by Equation (5.10) on page 33 and we are interested in the change of the free energy due to finite fluctuations of the n_z from $n_z = 0$. The change of the free energy under an arbitrary change of gap $\Delta_i \rightarrow \Delta_f$ is given by

$$\delta F = F_{\text{tot}, \Delta_f} - F_{\text{tot}, \Delta_i} + \frac{T}{2} \sum_{\mathbf{k}} \log \frac{1 - \exp\left(\sqrt{u^2 k^2 + \Delta_i^2}\right)}{1 - \exp\left(\sqrt{u^2 k^2 + \Delta_f^2}\right)}, \quad (\text{C.2})$$

where the first term is the free energy, which we would naively get from the path integral, which takes both branches into account and the last term corresponds to the aforementioned subtraction of the unphysical branch.

C.1 Application to the case of isotropically in-plane coupled impurities

The gap for isotropically impurities is computed in Equation (5.10) on page 33

$$\Delta = D \left(\frac{2J_{\perp} S \sqrt{1 - n_z^2 \rho K}}{D} \right)^{\frac{1}{2-k}}. \quad (\text{C.3})$$

If we expand the subtracted term in n_z we get

$$\delta F = \exp \left(-\frac{n_z^2}{2} \sum_{\mathbf{k}} \frac{\Delta^2}{T\sqrt{u^2 k^2 + \Delta^2}} \right) = \exp \left[-\frac{n_z^2}{2} \Delta^2 \log \left(\frac{D}{\Delta} \right) \right], \quad (\text{C.4})$$

which is exactly the term, which we expected to get, judging from the fermionic calculation in Chapter 2.

C.2 Application to the case of anisotropically in-plane coupled impurities

Analogously, using the gap, which includes the anisotropy terms

$$\Delta = D \left(\frac{2J_{\perp} S \sqrt{1 - n_z^2} [1 + \epsilon(x) e^{i2\alpha(x,\tau)} + \epsilon^*(x) e^{-i2\alpha(x,\tau)}] \rho K}{D} \right)^{\frac{1}{2-K}} \quad (\text{C.5})$$

and expanding in both n_z and $\epsilon(x)$, $\epsilon^*(x)$ one gets

$$\delta F = \exp \left[\left(-\frac{n_z^2}{2} \epsilon(x) e^{i2\alpha(x,\tau)} + \epsilon^*(x) e^{-i2\alpha(x,\tau)} \right) 2\Delta^2 \log \left(\frac{D}{\Delta} \right) \right]. \quad (\text{C.6})$$

List of Figures

1.1	Chiral edge states of a quantum Hall device (Source: [16])	3
1.2	Unit cell of Graphene (Source: [9])	5
1.3	Brillouin zone of Graphene (Source: [9])	5
1.4	Electronic dispersion between two boundary Kramers degenerate points. In the left the number of surface states crossing the Fermi energy is even, whereas in the right panel it is odd. (Source: [10])	9
2.1	Kondo impurity on the edge of a quantum spin Hall insulator (Source: PRB 84 195310 (2011))	12
2.2	Backscattering is only possible with a flip of the spins of the electron and the impurity	13
2.3	Forward scattering is only possible without flipping any spins	13
2.4	RG flow of the Kondo model in a helical edge state (Source:[35])	14
2.5	Physical picture of the Kondo singlet fixed point in a helical edge state (Source: [25])	14
2.6	Real and imaginary parts of correction to conductance at different temperatures (Source: [32])	17
2.7	Localized magnetic impurities interact with edge states of a quantum spin Hall insulator (Source: [2])	18
2.8	Ordering of the Kondo impurities by electronically mediated exchange interactions, induce a separation of lengthscales	19
4.1	RG flow for the density of magnetic impurities embedded into a helical edge liquid (Source: [24])	30
5.1	Plot of the gap for $0 < K < 2$	33
5.2	Spectrum of the gapped bosons, the lower branch of the spectrum is unphysical	34
6.1	Plot of $\frac{T_K}{100D}$ for $J_{\perp} = 0.01$ (limit of $1 - K \gg J_{\perp}$)	38
6.2	Phase diagram of the helical edge state with Kondo impurities	39
A.1	Comparison between single particle excitations in (a) higher dimensions and (b) one dimension (Source: [12])	43

List of Figures

A.2 Possible interaction processes in an helical edge liquid 48

Bibliography

- [1] Abrahams, E. ; Anderson, P.W. ; Licciardello, D.C. ; Ramakrishnan, T.V.: Scaling Theory of Localization: Absence of Quantum Diffusion in Two Dimensions. In: *Physical Review Letters* 42, Nr. 10, S. 673–676
- [2] Altshuler, B. L. ; Aleiner, I. L. ; Yudson, V. I.: Localization at the Edge of a 2D Topological Insulator by Kondo Impurities with Random Anisotropies. In: *Physical Review Letters* 111 (2013), Nr. 8
- [3] Bernevig, B. A. ; Hughes, T. L.: *Topological insulators and topological superconductors*. Princeton University Press, 2013. – ISBN 9780691151755
- [4] Bernevig, B. A. ; Hughes, T. L. ; Zhang, S. C.: Quantum spin Hall effect and topological phase transition in HgTe quantum wells. In: *Science* 314 (2006), Nr. 5806, S. 1757–61
- [5] Cardy, J. L.: *Scaling and renormalization in statistical physics*. Cambridge; New York : Cambridge University Press, 1996. – ISBN 9780521499590
- [6] Cheianov, V. ; Glazman, L. I.: Mesoscopic fluctuations of conductance of a helical edge contaminated by magnetic impurities. In: *Phys Rev Lett* 110 (2013), Nr. 20, S. 206803
- [7] Emery, V. J. ; Kivelson, S.: Mapping of the two-channel Kondo problem to a resonant-level model. In: *Phys Rev B Condens Matter* 46 (1992), Nr. 17, S. 10812–10817
- [8] Emery, V. J. ; Kivelson, S. A.: Solution of an orbital Kondo array. In: *Phys Rev Lett* 71 (1993), Nr. 22, S. 3701–3704
- [9] Fradkin, E.: *Field theories of condensed matter physics*. Cambridge Univ. Press, 2013. – ISBN 9781107308336
- [10] Franz, M. ; L., Molenkamp: *Topological Insulators*. Elsevier Science, 2013. – ISBN 9780444633149
- [11] Furusaki, A. ; Nagaosa, N.: Kondo effect in a Tomonaga-Luttinger liquid. In: *Phys Rev Lett* 72 (1994), Nr. 6, S. 892–895

- [12] Giamarchi, T.: *Quantum physics in one dimension*. Oxford; New York : Clarendon ; Oxford University Press, 2004. – ISBN 9780198525004
- [13] Giamarchi, T. ; Schulz, H. J.: Anderson localization and interactions in one-dimensional metals. In: *Phys Rev B Condens Matter* 37 (1988), Nr. 1, S. 325–340
- [14] Gulacsi, M.: The one-dimensional Kondo lattice model at partial band filling. In: *Advances in Physics* 53 (2004), Nr. 7, S. 769–937
- [15] Hasan, M. Z. ; Kane, C. L.: Colloquium: Topological insulators. In: *Reviews of Modern Physics* 82 (2010), Nr. 4, S. 3045–3067
- [16] Kane, C. L.: Chapter 1 - Topological Band Theory and the \mathbb{Z}_2 Invariant. In: Franz, M. (Hrsg.) ; Molenkamp, L. (Hrsg.): *Contemporary Concepts of Condensed Matter Science - Topological Insulators* Bd. 6. Elsevier, 2013. – ISBN 15720934, S. 3–34
- [17] Kane, C. L. ; Mele, E. J.: Quantum spin Hall effect in graphene. In: *Phys Rev Lett* 95 (2005), Nr. 22, S. 226801
- [18] Kane, C. L. ; Mele, E. J.: \mathbb{Z}_2 topological order and the quantum spin Hall effect. In: *Phys Rev Lett* 95 (2005), Nr. 14, S. 146802
- [19] Kittel, C.: *Quantum theory of solids*. New York : Wiley, 1963. – ISBN 9780471825630
- [20] Klitzing, K. ; Dorda, G. ; Pepper, M.: New Method for High-Accuracy Determination of the Fine-Structure Constant Based on Quantized Hall Resistance. In: *Physical Review Letters* 45 (1980), Nr. 6, S. 494–497
- [21] Konig, M. ; Wiedmann, S. ; Brune, C. ; Roth, A. ; Buhmann, H. ; Molenkamp, L. W. ; Qi, X. L. ; Zhang, S. C.: Quantum spin hall insulator state in HgTe quantum wells. In: *Science* 318 (2007), Nr. 5851, S. 766–70
- [22] Landau L.D., Lifshic E.M. Pitaevskij L.: *Statistical physics. Part 1*. 1980. – ISBN 9780080230399
- [23] Lee, D. H. ; Toner, J.: Kondo effect in a Luttinger liquid. In: *Phys Rev Lett* 69 (1992), Nr. 23, S. 3378–3381
- [24] Maciejko, J.: Kondo lattice on the edge of a two-dimensional topological insulator. In: *Physical Review B* 85 (2012), Nr. 24

- [25] Maciejko, J. ; Liu, C. ; Oreg, Y. ; Qi, X. L. ; Wu, C. ; Zhang, S. C.: Kondo effect in the helical edge liquid of the quantum spin Hall state. In: *Phys Rev Lett* 102 (2009), Nr. 25, S. 256803
- [26] Moore, J. E. ; Balents, L.: Topological invariants of time-reversal-invariant band structures. In: *Physical Review B* 75 (2007), Nr. 12
- [27] Qi, X.-L.: Chapter 4 - Field-Theory Foundations of Topological Insulators. In: Franz, M. (Hrsg.) ; Molenkamp, L. (Hrsg.): *Contemporary Concepts of Condensed Matter Science - Topological Insulators* Bd. 6. Elsevier, 2013. – ISBN 15720934, S. 91–122
- [28] Qi, X. L. ; Wu, Y. S. ; Zhang, S. C.: Topological quantization of the spin Hall effect in two-dimensional paramagnetic semiconductors. In: *Physical Review B* 74 (2006), Nr. 8
- [29] Qi, X. L. ; Zhang, S. C.: Topological insulators and superconductors. In: *Reviews of Modern Physics* 83 (2011), Nr. 4, S. 1057–1110
- [30] Roy, R.: Z₂ classification of quantum spin Hall systems: An approach using time-reversal invariance. In: *Physical Review B* 79 (2009), Nr. 19
- [31] Semenoff, G.: Condensed-Matter Simulation of a Three-Dimensional Anomaly. In: *Physical Review Letters* 53 (1984), Nr. 26, S. 2449–2452
- [32] Tanaka, Y. ; Furusaki, A. ; Matveev, K. A.: Conductance of a helical edge liquid coupled to a magnetic impurity. In: *Phys Rev Lett* 106 (2011), Nr. 23, S. 236402
- [33] Thouless, D. J. ; Kohmoto, M. ; Nightingale, M. P. ; Denny, M.: Quantized Hall Conductance in a Two-Dimensional Periodic Potential. In: *Physical Review Letters* 49 (1982), Nr. 6, S. 405–408
- [34] Wen, X.-G.: *Quantum field theory of many-body systems: From the origin of sound to an origin of light and electrons*. Oxford University Press, 2004. – ISBN 9780191523960 0191523968
- [35] Wu, C. ; Bernevig, B. A. ; Zhang, S. C.: Helical liquid and the edge of quantum spin Hall systems. In: *Phys Rev Lett* 96 (2006), Nr. 10, S. 106401
- [36] Xu, C. ; Moore, J.: Stability of the quantum spin Hall effect: Effects of interactions, disorder, and Z₂ topology. In: *Physical Review B* 73 (2006), Nr. 4
- [37] Yakovenko, V.: Chern-Simons Terms and n Field in Haldane's Model for the Quantum Hall Effect without Landau Levels. In: *Physical Review Letters* 65 (1990), Nr. 2, S. 251–254

- [38] Zachar, O. ; Kivelson, S. A. ; Emery, V. J.: Exact Results for a 1D Kondo Lattice from Bosonization. In: *Phys Rev Lett* 77 (1996), Nr. 7, S. 1342–1345